The Journal of Experimental Biology 207, 1163-1182
Published by The Company of Biologists 2004
doi:10.1242/jeb.00856

The anterior cardiac plexus: an intrinsic neurosecretory site within the stomatogastric nervous system of the crab *Cancer productus*

Andrew E. Christie[1,2,*], Shaun D. Cain[2], John M. Edwards[1,2], Todd A. Clason[1], Elena Cherny[1], Minhui Lin[2], Amitoz S. Manhas[2], Kirsten L. Sellereit[2], Nicholas G. Cowan[2], Kellen A. Nold[2], Hans-Peter Strassburg[2] and Katherine Graubard[1,2]

[1]*Department of Biology, University of Washington, Box 351800, Seattle, Washington 98195-1800 USA* and [2]*Friday Harbor Laboratories, University of Washington, 620 University Road, Friday Harbor, Washington 98250 USA*

*Author for correspondence at address 1 (e-mail: crabman@u.washington.edu)

Accepted 5 January 2004

Summary

The stomatogastric nervous system (STNS) of decapod crustaceans is modulated by both locally released and circulating substances. In some species, including chelate lobsters and freshwater crayfish, the release zones for hormones are located both intrinsically to and at some distance from the STNS. In other crustaceans, including Brachyuran crabs, the existence of extrinsic sites is well documented. Little, however, is known about the presence of intrinsic neuroendocrine structures in these animals. Putative intrinsic sites have been identified within the STNS of several crab species, though ultrastructural confirmation that these structures are in fact neuroendocrine in nature remains lacking. Using a combination of anatomical techniques, we demonstrate the existence of a pair of neurosecretory sites within the STNS of the crab *Cancer productus*. These structures, which we have named the anterior cardiac plexi (ACPs), are located on the anterior cardiac nerves (*acn*s), which overlie the cardiac sac region of the foregut. Each ACP starts several hundred μm from the origin of the *acn* and extends distally for up to several mm. Transmission electron microscopy done on these structures shows that nerve terminals are present in the peripheral portion of each *acn*, just below a well defined epineurium. These terminals contain dense-core and, occasionally, electron-lucent vesicles. In many terminals, morphological correlates of hormone secretion are evident. Immunocytochemistry shows that the ACPs are immunopositive for FLRFamide-related peptide. All FLRFamide labeling in the ACPs originates from four axons, which descend to these sites through the superior oesophageal and stomatogastric nerves. Moreover, these FLRFamide-immunopositive axons are the sole source of innervation to the ACPs. Collectively, our results suggest that the STNS of *C. productus* is not only a potential target site for circulating hormones, but also serves as a neuroendocrine release center itself.

Key words: incident light microscopy, transmission electron microscopy, laser scanning confocal microscopy, FLRFamide-related peptide, neurohormone, neuromodulation, crab, *Cancer productus*.

Introduction

Crustacean preparations have provided many insights into neuroendocrine function. Long before the concept of neurosecretion was formally demonstrated in vertebrates, several authors had independently described the neurohemal function of sites within the nervous system of crabs (Bliss, 1951; Passano, 1951). While many definitions of a neuroendocrine site exist, in the broadest of terms, it is generally accepted to be a region in which nerve terminals come in contact with the circulatory system (Cooke and Sullivan, 1982). Given this definition, many regions of the crustacean nervous system are likely to contribute to the hormone complement present in the hemolymph. Most crustacean neuroendocrine sites appear as rather unorganized regions of secretory terminals within or just below the sheath of nerves and ganglia (Friend, 1976; King, 1976; Sullivan et al., 1977; Livingstone et al., 1981; Kobierski et al., 1987; Kilman and Marder, 1996; Kilman, 1998; Skiebe et al., 1999; Skiebe and Ganeshina, 2000). Others, however, are more formally delimited, giving rise to what are often termed neurosecretory organs (Bliss, 1951; Passano, 1951; Alexandrowicz and Carlisle, 1953; Carlisle and Knowles, 1959; Maynard, 1961a,b; Maynard and Maynard, 1962; Cooke and Sullivan, 1982).

Small molecule transmitters, biogenic amines, peptides, and diffusible gases have been identified in crustacean neuroendocrine sites (Evans et al., 1976; Beltz and Kravitz, 1983; Schwarz et al., 1984; Siwicki et al., 1985, 1987; Siwicki and Bishop, 1986; Stangier et al., 1986, 1988; Kobierski et al.,

1987; Dircksen, 1992; Rodriguez-Sosa et al., 1994; Christie et al., 1995, 2003; Wood et al., 1996; Chang et al., 1999; Skiebe et al., 1999, 2002; Yang et al., 1999; Lee et al., 2000; Wang et al., 2000). These bioactive agents affect many target tissues and have been shown to directly control or influence a variety of physiological processes such as molting, metamorphosis, color change and the regulation of hemolymph glucose levels (Huberman, 1990; Keller, 1992; Rao, 1992; Rao and Riehm, 1993; Chang, 1993; Wainwright et al., 1996; Fingerman, 1997; Fingerman et al., 1998; Soyez, 1997; Chung et al., 1999; Phlippen et al., 2000). Circulating hormones have also been implicated in numerous aspects of nervous system function, including modulation of the neural circuits and muscles involved in feeding-related behavior (Turrigiano and Selverston, 1989, 1990; Heinzel et al., 1993; Marder et al., 1994, 1995; Christie and Nusbaum, 1995, 1998; Jorge-Rivera and Marder, 1996, 1997; Jorge-Rivera, 1997; Jorge-Rivera et al., 1998; Weimann et al., 1997).

In crustaceans, the stomatogastric nervous system (STNS; Fig. 1), an extension of the central nervous system, controls the ingestion and movement of food through the foregut (Selverston and Moulins, 1987; Harris-Warrick et al., 1992). Four ganglia are contained within the STNS: the stomatogastric ganglion (STG), the oesophageal ganglion (OG) and the paired commissural ganglia (CoGs). A number of nerves connect these ganglia and/or innervate the muscles of the foregut. Several distinct, but interacting, neural circuits are present within the STNS, including one contained within the STG that produces both the pyloric and gastric mill rhythms (Selverston and Moulins, 1987; Harris-Warrick et al., 1992). Multiple forms of the pyloric and gastric mill motor patterns have been shown to exist (Selverston and Moulins, 1987; Harris-Warrick et al., 1992; Marder et al., 1994, 1995, 1997; Marder and Calabrese, 1996; Skiebe, 2001). Research from many laboratories has shown that much of this flexibility is imparted through the actions of neuromodulators, including circulating hormones present in the hemolymph (Turrigiano and Selverston, 1990; Heinzel et al., 1993; Christie and Nusbaum, 1995, 1998; Weimann et al., 1997).

In many genera, particularly those of the infraorder Astacidea (chelate lobsters and freshwater crayfish), hormones released from both extrinsic and intrinsic sites are likely to influence the STNS. The extrinsic sites include some or all of the classically defined neuroendocrine organs, i.e. the sinus glands (SGs) of the eyestalk, the pericardial organs (POs) present in the venous cavity surrounding the heart, and the post-commissural organs (PCOs) located within the posterior commissure near the oesophagus (Cooke and Sullivan, 1982), as well as sites located on the second roots of the thoracic ganglia and on the ventral nerve cord (Livingstone et al., 1981; Kobierski et al., 1987).

Several neuroendocrine release zones within the STNS itself may also contribute to its hormonal modulation in lobsters and crayfish. One such site is an extensive plexus located within the sheath of the anterior portion of the STNS (Maynard and Dando, 1974; Kilman, 1998; Skiebe et al., 1999; Skiebe and Wollenschläger, 2002; Christie et al., 2003). While the extent of this structure remains undetermined in most species, in the American lobster *Homarus americanus*, and the Australian freshwater crayfish *Cherax destructor* and *Cherax quadricarinatus*, it is known to span the anterior portion of the stomatogastric nerve (*stn*) and all or a portion of the superior oesophageal (*son*), oesophageal, dorsal posterior oesophageal, inferior oesophageal and inferior ventricular nerves (Skiebe and Wollenschläger, 2002; Christie et al., 2003). In these species, transmission electron microscopy confirms the ultrastructure of the site to be neuroendocrine in nature (Kilman, 1998; Skiebe and Ganeshina, 2000; Christie et al., 2003). A second intrinsic neuroendocrine site is present on each circumoesophageal connective (*coc*) near the CoG (Skiebe et al., 1999). Like the plexus in the anterior portion of the STNS, this site is superficially located and has been shown to possess an ultrastructure consistent with a neuroendocrine release zone (Skiebe et al., 1999). Thus far this plexus has been identified in only one species, *C. destructor* (Skiebe et al., 1999). Additionally, in several species, including *H. americanus* and the California spiny lobster *Panulirus interruptus* (Infraorder Palinura), neuroendocrine profiles have been identified ultrastructurally in the sheath surrounding the STG and the nerves immediately adjacent to it, i.e. the *stn* and the dorsal ventricular nerve (Friend, 1976; King, 1976). These sites too may contribute to the hormonal control of the STNS.

As in lobsters and crayfish, the STNS of Brachyuran crabs is also modulated by hormones released from extrinsic neuroendocrine sites (Christie and Nusbaum, 1995, 1998; Weimann et al., 1997). Unlike the former groups, little is known about intrinsic neurosecretory zones in the STNS of these animals. Using incident light microscopy, Maynard and Dando (1974) identified an iridescent region on each of the paired anterior cardiac nerves (*acn*s) in the blue crab *Callinectes sapidus*. They interpreted this iridescence as indicative of a neurohemal release site. Similarly, Skiebe and Wollenschläger (2002), using antibodies to vesicle-associated proteins, identified putative neuroendocrine sites on the *acn*s of the European edible crab *Cancer pagurus*. In neither species is information available to confirm that the *acn* plexi are ultrastructurally identifiable as neuroendocrine release zones.

In the present study, we used incident light microscopy to survey the STNS of the red rock crab *Cancer productus* for putative neuroendocrine sites. As with *C. sapidus* and *C. pagurus* (Maynard and Dando, 1974; Skiebe and Wollenschläger, 2002), the only putative neurosecretory sites identified were on the *acn*s. Using transmission electron microscopy, we confirmed that these sites, which we have named the anterior cardiac plexi or ACPs, are ultrastructurally identifiable as neuroendocrine release zones. All innervation to the ACPs originates from four axons that project to the plexi *via* the *stn* and *son*s. Modulator immunolabeling shows that all four of the axons innervating the ACPs exhibit FLRFamide-related peptide immunoreactivity. Our confirmation of the ACPs of *C. productus* as neuroendocrine plexi shows that intrinsic neurosecretory sites exist in the STNS of this species.

This finding strengthens the hypothesis that the *acn* sites previously identified in *C. sapidus* (Maynard and Dando, 1974) and *C. pagurus* (Skiebe and Wollenschläger, 2002) are also neuroendocrine in nature. Moreover, our results set the stage for future biochemical and physiological studies of the ACPs, the hormones contained within them and their actions on potential target tissues. Some of this data has appeared previously in abstract form (Christie et al., 2002).

Materials and methods

Animals and tissue dissection

Cancer productus Randall (*N*=47 animals) were hand collected at multiple locations in the greater Puget Sound area of Washington State (USA) or purchased from Coastal Catch (Santa Barbara, California, USA). All animals were maintained either in aerated natural seawater aquaria chilled to approximately 10°C (Department of Biology, University of Washington, Seattle, Washington, USA) or in flow-through natural seawater tanks (Friday Harbor Laboratories, Friday Harbor, Washington, USA; ambient water temperature approximately 10°C).

For tissue collection, crabs were anesthetized by packing in ice for 30–60 min, their foregut removed, and the STNS (Fig. 1) dissected from the foregut in chilled (approximately 4°C) physiological saline (440 mmol l^{-1} NaCl; 11 mmol l^{-1} KCl; 13 mmol l^{-1} $CaCl_2$; 26 mmol l^{-1} $MgCl_2$; 10 mmol l^{-1} Hepes acid, pH 7.4, adjusted with NaOH). Following dissection, tissue was pinned in a Sylgard 184 (KR Anderson, Santa Clara, California, USA)-lined Petri dish and subsequently processed as described below.

Incident light microscopy of living tissue

To examine fresh, unfixed tissue, the STNS was dissected as described above, then pinned flat in a Sylgard-lined Petri dish containing chilled (approximately 10°C) physiological saline. Preparations were viewed, and maps of the putative location of each ACP drawn, using either a Wild M5A (Heerbrugg, Switzerland) or Nikon SMZ1000 (Tokyo, Japan) stereomicroscope with illumination provided by a Fiber-Lite Model 190 fiber optic illuminator (Dolan-Jenner Industries, Inc., Woburn, Massachusetts, USA). Each preparation was examined at multiple magnifications. The illuminating beam was adjusted several times at each magnification so as to allow the tissue to be examined at multiple illuminating angles. Incident light micrographs were taken using a CoolSNAP camera system (Roper Scientific, Inc., Tucson, Arizona, USA) mounted on the Nikon microscope.

Light and transmission electron microscopy

For light level and transmission electron microscopy, methods modified from standard techniques were used (Dircksen, 1992; Kilman and Marder, 1996; Kilman, 1998; Webster et al., 2000). Specifically, ACPs were identified using incident light microscopy (see above) and subsequently isolated. These stretches of the *acn* were fixed using one of two

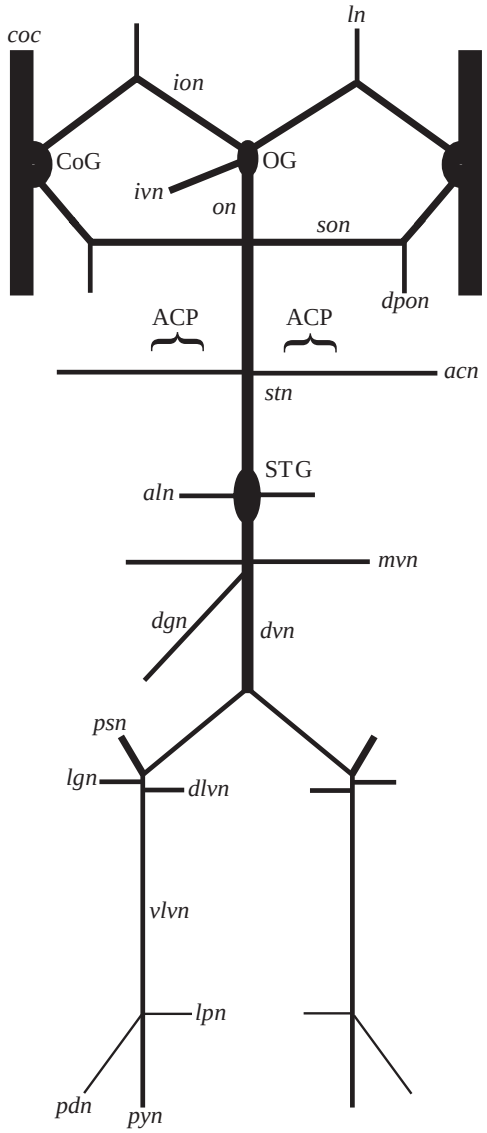

Fig. 1. Schematic representation of the stomatogastric nervous system, including the location of the anterior cardiac plexi (ACPs). The paired ACPs are located on the anterior cardiac nerves (*acn*s) which overlie the cardiac sac region of the foregut. *aln*, anterior lateral nerve; *coc*, circumoesophageal connective; CoG, commissural ganglion; *dgn*, dorsal gastric nerve; *dlvn*, dorsal lateral ventricular nerve; *dpon*, dorsal posterior oesophageal nerve; *dvn*, dorsal ventricular nerve; *ion*, inferior oesophageal nerve; *ivn*, inferior ventricular nerve; *lgn*, lateral gastric nerve; *ln*, labral nerve; *lpn*, lateral pyloric nerve; *lvn*, lateral ventricular nerve; *mvn*, medial ventricular nerve; OG, oesophageal ganglion; *on*, oesophageal nerve; *pdn*, pyloric dilator nerve; *psn*, pyloric sensory nerve; *pyn*, pyloric nerve; *son*, superior oesophageal nerve; STG, stomatogastric ganglion; *stn*, stomatogastric nerve; *vlvn*, ventral lateral ventricular nerve.

protocols. In the first protocol, *acn*s were fixed for 1–2 h at 4°C in freshly prepared Karnovsky's fixative [2.5% glutaraldehyde (EM grade; Electron Microscopy Sciences, Fort Washington, Pennsylvania, USA), 2% paraformaldehyde (EM grade; Electron Microscopy Sciences), 0.1% $CaCl_2$ and 5% sucrose

in 0.2 mol l^{-1} sodium cacodylate buffer, pH 7.2], rinsed twice (at 15 min intervals) in sodium cacodylate buffer and then post-fixed for 1 h with 1% OsO_4 in sodium cacodylate buffer. Following post-fixation, tissue was rinsed twice in sodium cacodylate buffer (at 15 min) and subsequently dehydrated in a graded ethanol series (40%, 60%, 80%, 95% and 100%). Dehydrated tissue was passed through an ethanol/LX-112 epoxy resin (Ladd Research Industries, Williston, Vermont, USA) series (3:1, 1:1, 1:3; 90 min each) and then left in 100% LX-112 overnight. After this overnight infiltration, tissue was transferred to embedding molds filled with fresh LX-112 and polymerized at 60°C for 8 h.

In the second protocol, *acn*s were fixed overnight in 4% paraformaldehyde, 0.1% glutaraldehyde in 0.1 mol l^{-1} sodium phosphate (P) buffer (pH 7.4) at 4°C. Following fixation, tissue was rinsed twice in P buffer (at 10 min intervals) and subsequently post-fixed in 1% OsO_4 in 0.01 mol l^{-1} sodium phosphate buffer, pH 7.4. Following post-fixation, tissue was rinsed twice in distilled water (at 10 min intervals) and then dehydrated in graded ethanol series (see above). Some tissue fixed *via* this second protocol was embedded in LRWhite (LRW) resin (Electron Microscopy Sciences). Here, tissue was taken from ethanol into 100% activated LRW for 2 h. Tissue was subsequently transferred to fresh LRW overnight and then transferred again to fresh LRW for 2 h. Tissue was then embedded in fresh LRW using #1 gelatin capsules (Ted Pella, Redding, California, USA) and polymerized at 45°C for 48 h. The remaining *acn*s fixed *via* the second protocol were taken from ethanol into a 1:1 mix of ethanol:propylene oxide for 30 min. Tissue was then rinsed twice in propylene oxide (at 15 min intervals), transferred into a 1:1 mix of propylene oxide:100% EMBed (EMB) resin (Electron Microscopy Sciences) for 2 h and then into fresh EMB for 2 h. After 2 h, the resin was replaced with fresh EMB and allowed to infiltrate overnight. After this overnight infiltration, tissue was again transferred to fresh EMB for 2 h and subsequently polymerized in fresh EMB for 48 h at 45°C.

Regardless of the resin used, polymerized blocks were sectioned for light microscopy at 1.0 μm using glass knives and for transmission electron microscopy at 70–90 nm with a diamond knife (Diatome, Fort Washington, Pennsylvania, USA). All sectioning was done using a RMC MT6000 ultramicrotome (Research and Manufacturing Company Inc., Tucson, Arizona, USA). Sections used for light microscopic analysis were mounted on glass microscope slides and subsequently stained with 1% Toluidine Blue, 1% borax in distilled water for 60 s at 60°C. Micrographs were taken with a Nikon CoolPix 4500 digital camera mounted on a Nikon Eclipse E800 microscope using a PlanFluor 40× 1.35NA oil immersion lens. For transmission electron microscopy, sections were mounted on copper mesh grids and stained with 4% uranyl acetate and Reynolds' lead citrate (Reynolds, 1963) for 1 h and 30 s, respectively. Tissue was examined and micrographs generated using a Philips CM100 transmission electron microscope (Philips Electronic Instrument Company, Mahwah, New Jersey, USA) at 60 kV.

The gross ultrastructure of the *acn* was the same regardless of the tissue processing used.

Wholemount immunocytochemistry

For wholemount immunocytochemistry, tissue was fixed overnight in freshly made 4% paraformaldehyde in P buffer (pH 7.4; see above for composition). Fixed tissue was rinsed five times over approximately 5 h in a solution of P buffer containing 0.3% Triton X-100 (P-Triton). Incubation in primary antibody (or antibodies) was done in P-Triton, with 10% normal goat serum (NGS) added to diminish nonspecific binding. Following incubation in primary antibody, tissues were again rinsed five times over approximately 5 h in P-Triton and then incubated in secondary antibody (or antibodies). As with the primary antibody, secondary antibody incubation was done in P-Triton with 10% NGS. After secondary antibody incubation, each preparation was rinsed five times over approximately 5 h in P buffer and then mounted between a glass microscope slide and coverslip using either a solution of 80% glycerine, 4% *n*-propyl gallate (pH ~9.0) or Vectashield mounting medium (Vector Laboratories, Inc., Burlingame, California, USA). Fixation and incubation in both primary and secondary antibody were done at 4°C. Incubation in both primary and secondary antibody was done using gentle agitation. All rinses were done at room temperature without agitation. Secondary antibody incubation and all subsequent processing was conducted in the dark. Likewise, slides were stored in the dark at 4°C until examined.

Antibodies

To determine whether FLRFamide-related peptides were present in the ACPs, we used a rabbit polyclonal antibody generated against FMRFamide (catalog #20091; Immunostar Inc., Hudson, Wisconsin, USA). This antibody was chosen as it has been used previously for mapping the distribution of this peptide family in several crustacean species (Schmidt and Ache, 1994a,b; Tierney et al., 1997; Fénelon et al., 1998; Blitz et al., 1999; Kilman et al., 1999; Meyrand et al., 2000). As all known crustacean FMRFamide-related peptides contain the carboxy-terminal amino acid sequence FLRF rather than FMRF (Trimmer et al., 1987; Krajniak, 1991; Mercier et al., 1993; Weimann et al., 1993), in this paper we will refer to the FMRF antibody and its immunolabeling as FLRFamide antibody and immunolabeling, respectively. In our study the FLRFamide antibody was used at a final dilution of 1:300 with an incubation time of 48–72 h.

As a general marker for electron-lucent vesicles (ELVs), an antibody generated against the synaptic vesicle-associated protein synapsin was used. This antibody is a mouse monoclonal antibody generated against a glutathione S-transferase fusion protein, which includes a portion of a *Drosophila* synapsin homolog (SYNORF1; Klagges et al., 1996; provided for this study by E. Buchner). This antibody has been used previously to identify the location of putative synaptic neuropil and neurosecretory sites in several crustaceans (Skiebe, 2000; Skiebe and Ganeshina, 2000;

Skiebe and Wollenschläger, 2002). In our study, the synapsin antibody was used at a final dilution of 1:20 with an incubation time of approximately 72 h.

The secondary antibodies used in our study were goat anti-rabbit IgG labeled with Texas Red (catalog #111-075-144; Jackson ImmunoResearch Corporation, West Grove, Pennsylvania, USA) and goat anti-mouse IgG labeled with FITC (catalog #115-095-146; Jackson ImmunoResearch Corporation). Both antibodies were used at final dilutions of 1:300 with incubation times of 12–24 h.

Preadsorption controls

To strengthen our confidence that the FLRFamide immunoreactivity seen in the ACP was due to the presence of FLRFamide-related peptides, we conducted a series of preadsorption controls. In these experiments, TNRNFLRFamide (American Peptide Company, Sunnyvale, California, USA), SDRNFLRFamide (American Peptide Company), *Cancer borealis* tachykinin related-peptide Ia (APSGFLGMRamide; synthesized by the Protein Chemistry Laboratory, University of Pennsylvania School of Medicine, University of Pennsylvania, Philadelphia, Pennsylvania, USA, and provided for this study by M. Nusbaum), or proctolin (RYLPT; Peninsula Laboratories, Belmont, California, USA) were used as blocking agents. In each experiment, the FLRFamide antibody was incubated with a blocking agent for 2 h at room temperature prior to applying the solution to the tissue. Immunoprocessing was then performed as described above. TNRNFLRFamide and SDRNFLRFamide were chosen for these experiments as they are the only FLRFamide-related peptides thus far isolated from crabs of the genus *Cancer* (Weimann et al., 1993). *Cancer borealis* tachykinin related-peptide Ia and proctolin were chosen as they too are known to be present in species of the genus *Cancer* in their native form (Marder et al., 1986; Christie et al., 1997b).

Lucifer Yellow nerve backfilling

In some experiments, one *acn* was backfilled with Lucifer Yellow-CH dilithium salt (LY; Sigma; Saint Louis, Missouri, USA or Molecular Probes, Eugene, Oregon, USA) prior to fixation and FLRFamide immunoprocessing. In these experiments, a Vaseline well was built around the *acn* and the saline within the well subsequently replaced with distilled water. After several minutes, the distilled water was removed and replaced with a solution of 10–20% LY in distilled water and the nerve was transected within the well. Following transection, the preparation was incubated at 10°C for 18–72 h in the dark. Dye was subsequently removed from the well and the preparation fixed and immunolabeled as described above. All immunoprocessing of LY backfilled preparations was done in the dark.

Confocal and epifluorescense microscopy

All fluorescent preparations, regardless of the type of processing, were viewed and data collected using one of two Bio-Rad MRC 600 laser scanning confocal microscopes (Bio-Rad Microscience Ltd., Hemel Hempstead, UK), a Bio-Rad Radiance 2000 laser scanning confocal microscope or a Nikon Eclipse E600 epifluorescense microscope. The Bio-Rad MRC 600 system located at the University of Washington (Department of Biology) is equipped with a Nikon Optiphot upright microscope and a krypton/argon mixed gas laser. Nikon Fluor 10× 0.5NA dry, PlanApo 20× 0.75NA dry and PlanApo 60× 1.4NA oil immersion lenses were used for imaging. Bio-Rad supplied YHS or K1/K2 filter sets and Comos software were used for imaging all preparations on this system (filter specifications are as described in Christie et al., 1997a). The Bio-Rad MRC 600 system located at Friday Harbor Laboratories is equipped with a Nikon Optiphot inverted microscope and uses the same laser, filters and software as the MRC 600 system located at the University of Washington. With the addition of a Nikon Fluor 40× 0.85NA dry lens, the objective lenses were also the same as those located on the system at the University of Washington. The Bio-Rad Radiance 2000 laser scanning confocal microscope is equipped with a modified Nikon Eclipse E600FN microscope and a krypton/argon mixed gas laser. Nikon PlanApo 10× 0.45NA DIC dry, PlanApo 20× 0.75NA DIC dry and PlanApo 60× 1.4NA DIC oil immersion lenses were used for imaging. Bio-Rad supplied LaserSharp 2000 software and 560 DCLP dichroic and HQ 515/30 and E600LP emission filters were used for imaging tissue on this system. The Nikon Eclipse E600 epifluorescense microscope is equipped with Nikon PlanFluor 10× 0.30NA dry, PlanFluor 20× 0.50NA dry and PlanFluor 40× 0.75NA dry lenses and B-2E/C FITC (EX, 465–495 nm; DM, 505 nm; BA, 515–555 nm) and G-2E/C TRITC (EX, 528–553 nm; DM, 565 nm; BA, 600–660 mn) filter sets.

Figures were produced using a combination of Photoshop (version 7.0; Adobe Systems Inc., San Jose, California, USA) and Canvas (version 8.0; Deneba Systems Inc., Miami, Florida, USA) software. Contrast and brightness were adjusted as needed to optimize the clarity of the printed figures.

Results

Anatomical identification of the anterior cardiac plexi

Incident light survey of living tissue

Under incident illumination, crustacean neurosecretory sites typically exhibit a distinct bluish-white iridescence (Maynard and Maynard, 1962). This visual effect is attributed to the high density of peptide/amine-containing neurosecretory granules contained within these structures (Maynard and Maynard, 1962). To survey the STNS of *C. productus* for putative neurosecretory sites, we conducted an incident light examination of the entire STNS of this species. This included all ganglia, their interconnecting nerves and the major motor nerves of this system (Fig. 1). In each of the preparations examined (N=47 preparations), we observed a well delimited area of punctate, bluish-white iridescence on each of the paired *acn*s (Fig. 2A). On each *acn*, the iridescent region started close to the junction of this nerve and the *stn* and extended distally for up to several mm. The iridescent profiles present at this site

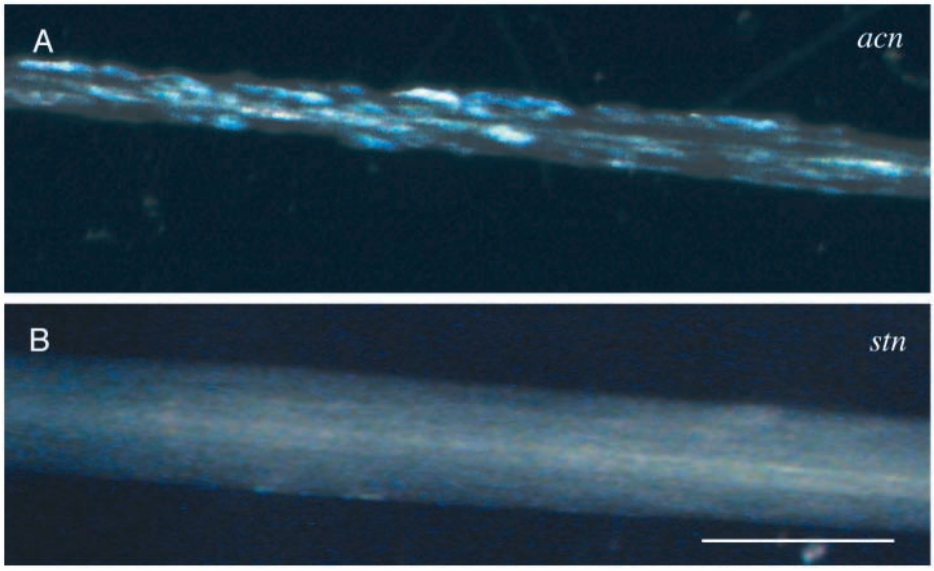

Fig. 2. Incident light micrographs of a portion of the anterior cardiac nerve (*acn*) and stomatogastric nerve (*stn*). (A) Incident light micrograph of the *acn*. This image, taken approximately 400 μm from the junction of the *acn* and the *stn* (see Fig. 1), shows numerous iridescent bluish-white profiles. These profiles appear superficially located and cover an approximately 1000 μm stretch of the nerve. (B) Incident light micrograph of the *stn*. In contrast to the *acn*, no iridescent profiles are seen in this nerve or in any other nerves (other than the *acn*s) or ganglia that comprise the stomatogastric nervous system. Scale bar, 100 μm.

appeared superficially located, within or just below the sheath of the nerve. In no other regions of the STNS did we consistently observe any distinct areas of iridescence within the sheath (Fig. 2B).

Light and transmission electron microscopy

To characterize the ultrastructure of the iridescent structures just described, we isolated several pieces of the *acn* (*N*=9 *acn*s) and subjected them to light and transmission electron microscopy. In each of these preparations, the iridescent region of the *acn* could be roughly divided into two parts: the central core and the peripheral zone. The central core of the *acn* was characterized by the presence of large (approximately 10 μm) diameter axons (Fig. 3A–C). All axons in the central core contained filamentous axoplasm and were tightly ensheathed by a thick wrapping of glia (Fig. 3D). Dense-core vesicles (DCVs) and ELVs were occasionally evident in these axons. At the end of the *acn* closest to the *stn*, five large diameter axons were present (Fig. 3A). Within the center of each *acn* segment, smaller diameter neurites emanated from the large fibers just described, radiating toward the periphery of the nerve (Fig. 3B). These neurites also showed glial wrapping and contained filamentous axoplasm as well as DCVs and, occasionally, ELVs. At the distal end of each *acn* segment, only one large diameter fiber was seen, suggesting that the other four axons terminate in the iridescent portion of the *acn* (Fig. 3C).

The peripheral portion of the *acn* was characterized by a distinctive epineurium, directly under which lie numerous nerve terminals and glial profiles (Fig. 4). The epineurium, which separates the nerve from the hemolymph space, was found to be composed of a moderately dense, amorphous material which was fenestrated with minute open spaces (Fig. 4B). This structure varied in thickness and completely ensheathed the nerve. Nerve terminals could often be seen to abut the epineurium, which frequently showed a marked thinning at these points of contact (data not shown). Clusters of terminals were common, with individual terminals often in direct apposition to one another with no intervening glial processes (Fig. 4B). The glia were irregular in shape with a relatively homogeneous cytoplasm. Glial protuberances often extended to the epineurium. Glial nuclei, with their distinctive chromatin arrangement, were also evident, usually, though not exclusively, at some distance from the epineurium (data not shown).

Fig. 3. Gross structure of the iridescent portion of anterior cardiac nerve (*acn*) and electron microscopy of its central core. (A–C) Light micrographs of Toluidine Blue-stained sections of the *acn*. These micrographs show that the iridescent portion of the *acn* can be divided into two parts, a central core containing large diameter axons (indicated numerically in A–C) and a peripheral region (see Figs 4 and 5). At the proximal end of the *acn* (A), five axons (labeled 1–5) are present. Regardless of preparation or fixation protocol, these axons are approximately 10 μm in major cross-sectional diameter. As one moves distally through the nerve (B), four of the five axons terminate into numerous smaller diameter axons (asterisks). The remaining axon (labeled 1 in B and C) maintains a constant diameter through the medial portion of the *acn*, ultimately exiting the iridescent portion of nerve (C). (D) Transmission electron micrograph of one of the five axons present in the central core of the *acn*. While taken from a distal section of an *acn* segment, the ultrastructure of this axon is typical of the ultrastructure of all axons present in the entire iridescent portion of the *acn*. Like all *acn* axons, the axon shown in this panel contains filamentous axoplasm (ap), mitochondria (m) and occasionally dense-core (DCV) and electron-lucent vesicles. In this micrograph, a single DCV is evident. This, and all other *acn* axons, is ensheathed by a thick glial wrap (gw). The glia contain a relatively homogeneous cytoplasm, often with mitochondria present. In this example, structures within the axon are labeled with black lettering while those associated with the glial wrap are labeled with white lettering. A, B and C are taken from different preparations. D is taken from the same preparation as C. Scale bars, 30 μm (A–C); 1 μm (D). It should be noted that the difference in appearance of the tissue in A *versus* B and C is due to the type of plastic used for embedding, namely LRWhite and EMBed, respectively.

The nerve terminals present at the periphery of the *acn* ranged in size from <1 μm to approximately 10 μm in major cross-sectional diameter and contained numerous DCVs as well as mitochondria and, occasionally, ELVs (Figs 4, 5). In no terminals were any conventional synapses seen. In many terminals, however, morphological correlates of hormone secretion were evident (Figs 4B, 5). These ultrastructural features included DCVs docked to the plasma membrane and omega (Ω)-figures (Fig. 5).

Based on their location and ultrastructure, we have named the above described neurosecretory region of each *acn* the anterior cardiac plexus or ACP.

FLRFamide labeling and sources of innervation of the anterior cardiac plexi

FLRFamide labeling

FLRFamide-related peptides have been shown to be present in many crustacean neuroendocrine sites (Kobierski et al., 1987; Krajniak, 1991; Mercier et al., 1993; Christie et al., 1995; Kilman, 1998; Skiebe et al., 1999; Pulver and Marder,

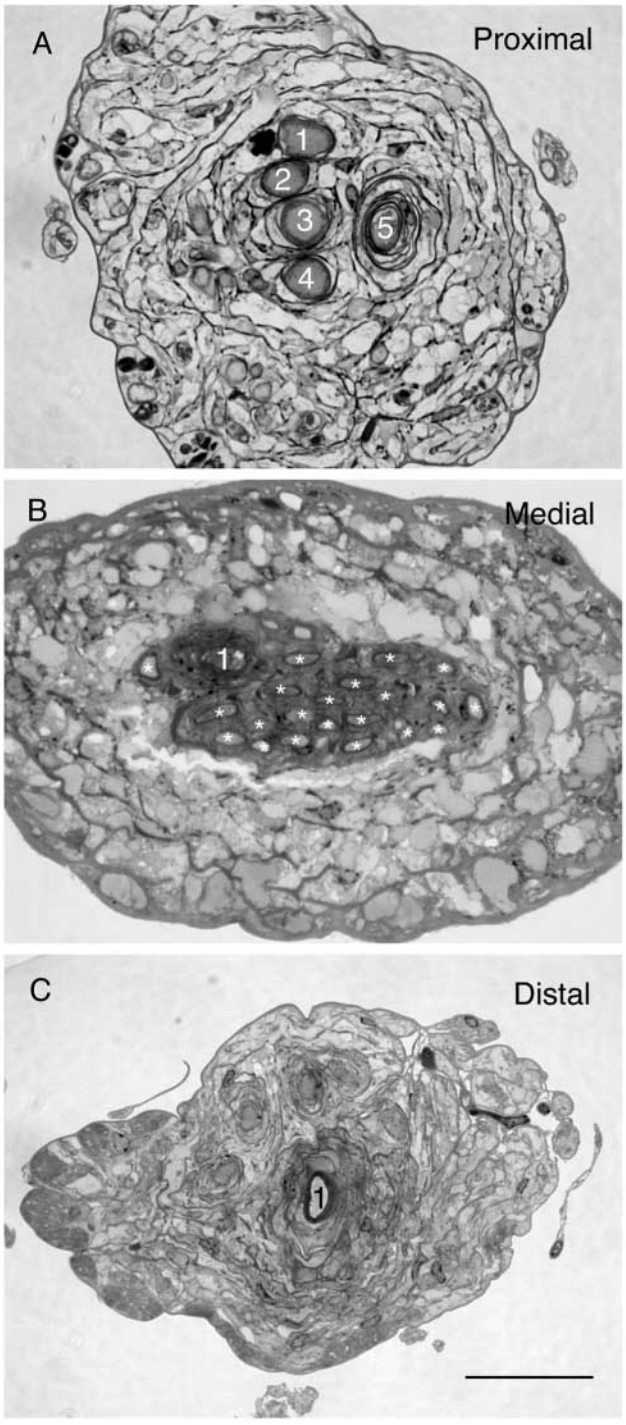

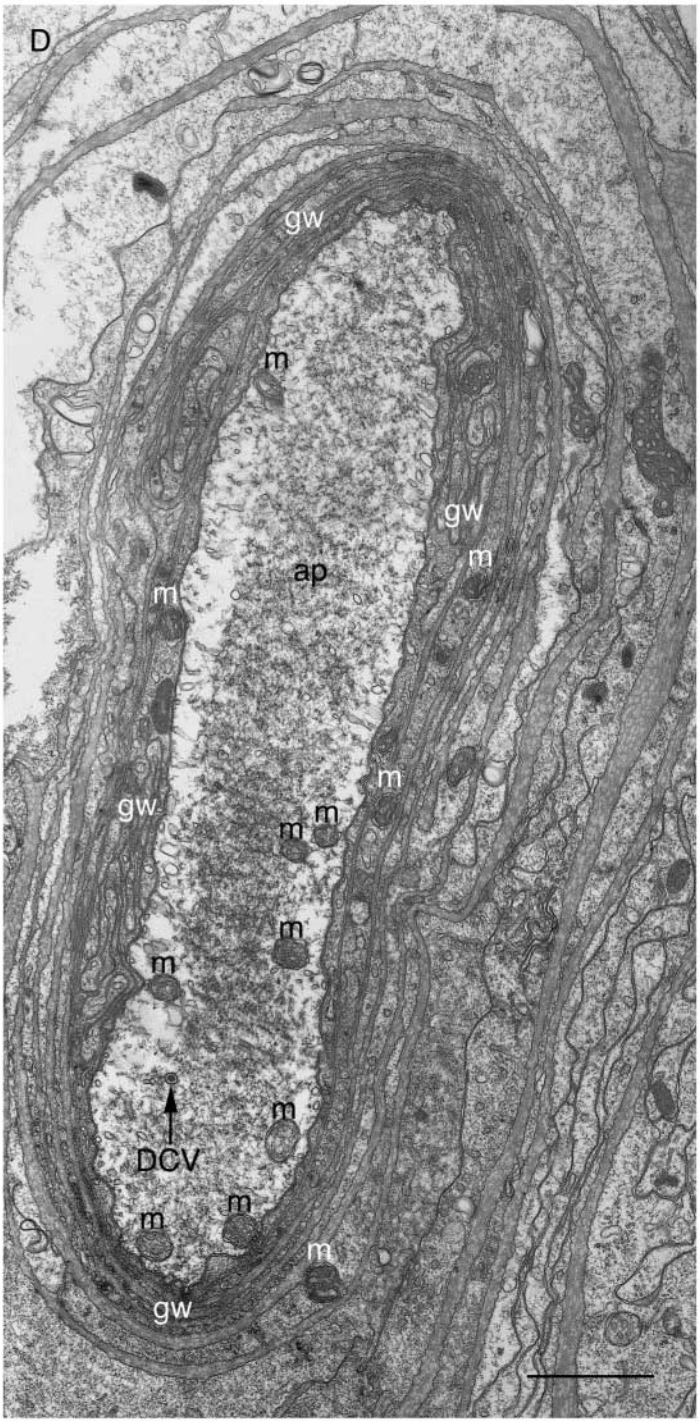

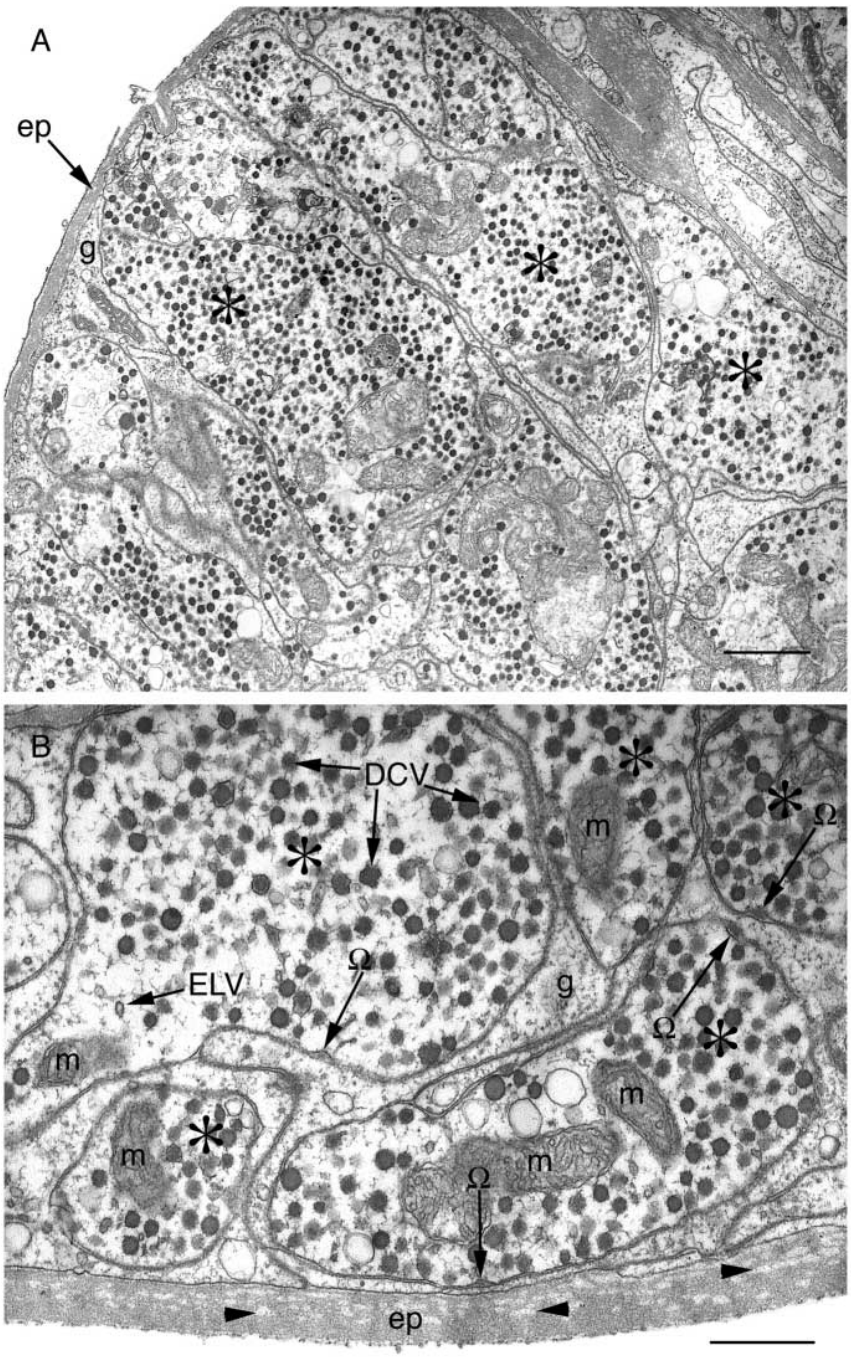

Fig. 4. Transmission electron microscopy of the peripheral portion of the anterior cardiac nerve (*acn*). (A) A low magnification micrograph of the periphery of the *acn*. An epineurium (ep) separates the nerve from the hemolymph space. Directly under the epineurium lie numerous nerve terminals, three of which are indicated with asterisks. Glial protuberances (g) are also present in the periphery of the *acn*. (B) A high magnification micrograph of the periphery of the *acn*. The epineurium is composed of a moderately dense, amorphous material that is fenestrated with minute open spaces (three of the larger fenestrations are indicated with black arrowheads). All or portions of five nerve terminals (asterisks) are present below the epineurium in this image. These terminals contain numerous dense-core vesicles (DCVs) and often mitochondria (m) and a small number of electron-lucent vesicles (ELVs). Morphological correlates of vesicle secretion, including vesicles docked to the plasma membrane and omega (Ω)-figures, are common on the nerve terminals. In this micrograph four Ω-figures are clearly visible. A and B are taken from the same preparation. Scale bars, 1 μm (A); 500 nm (B).

2002). To determine whether the ACP contains FLRFamide-related peptides, we conducted wholemount immunolabeling of the *acn*s (*N*=62 *acn*s). In each *acn*, intense FLRFamide immunoreactivity was seen in the portion of the nerve that contained the ACP. This label consisted both of immunopositive fibers and varicosities (Figs 6–9). In the region of the *acn* closest to *stn*, four FLRFamide-immunopositive fibers were present. After travelling distally for several hundred μm, these axons arborized, producing a large number of smaller diameter processes which radiated from the central core of the nerve, giving rise to a dense plexus of fine neurites studded with varicosities in the periphery (Figs 6, 7). The immunopositive varicosities varied widely both in shape and size (Fig. 7). These varicosities showed pronounced clustering in the perineural sheath region, which gives rise to a bark-like appearance of the immunolabel, particularly in the portion of the ACP closest to the *stn* (Fig. 8). Blister-like protuberances of the *acn* sheath were often seen in this region of the ACP. These protrusions commonly contained large numbers of tightly clustered FLRFamide-immunopositive varicosities (Fig. 9). No FLRFamide-like immunoreactivity was seen in any of the *acn*s past the plexi, which suggests that the four FLRFamide immunolabeled *acn* fibers terminate in the ACPs (Figs 6, 7).

Preadsorption controls

As our study is the first using the Immunostar FLRFamide antibody in *C. productus*, and the first time that any modulator staining has been reported in the ACP, we conducted experiments to confirm that the staining we report is suppressed specifically by preadsorption of the antibody with extended FLRFamide peptides. Incubation of the FLRFamide antibody with TNRNFLRFamide or SDRNFLRFamide (10^{-6} mol l^{-1}) completely abolished immunolabeling in the ACPs (*N*=6 ACPs for each peptide; data not shown). Staining in these structures after the FLRFamide antibody had been preincubated with either *Cancer borealis* tachykinin-related peptide Ia or proctolin (10^{-3} mol l^{-1}; *N*=6 ACPs for each peptide) was no different from antibody preincubations at room temperature with no blocking agent present (*N*=6 ACPs; data not shown).

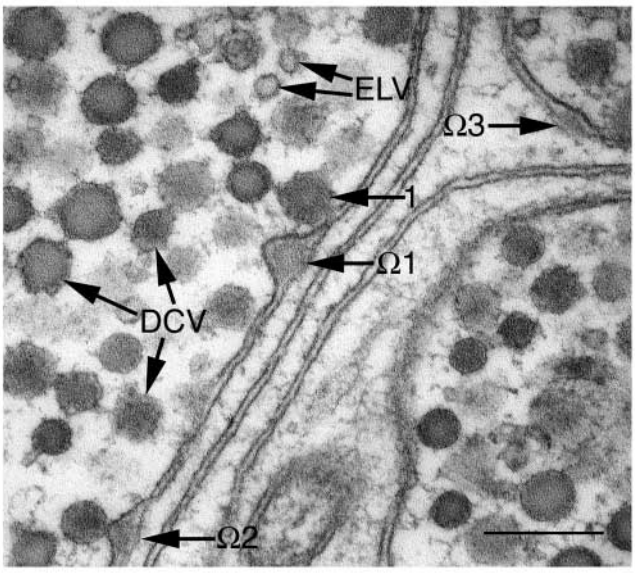

Fig. 5. Morphological correlates of hormone secretion are present in the anterior cardiac plexus. This transmission electron micrograph shows portions of several nerve terminals at high magnification. Both dense-core (DCV) and electron-lucent (ELV) vesicles are present in these terminals. In this image, one DCV is docked to the plasma membrane. Likewise, several DCVs have fused with the plasma membrane and are in the process of exocytosing their contents. This exocytosis creates characteristic ultrastuctural features on the plasma membrane commonly referred to as omega (Ω)-figures. The docked DCV and the three Ω-figures visible in this micrograph create a pseudo-time course of hormone secretion. First, a DCV docks to the plasma membrane (1) and subsequently fuses with it, releasing its dense-core and forming an Ω-figure (Ω1). The membrane of the DCV rapidly is incorporated into the plasma membrane of the terminal and the Ω-figure subsides (Ω2 and Ω3). Note that this micrograph is from a different preparation to that shown in Fig. 4. Scale bar, 200 nm.

Sources of FLRFamide innervation to the anterior cardiac plexi

As just described, four axons are the sole source of FLRFamide innervation to each ACP. In several preparations, including the one shown in Fig. 6A, the projection pathway of these fibers could be traced with relatively little ambiguity using the immunolabeling alone. In these preparations, two large diameter immunopositive axons in each *son* could be seen to project into the *stn* (for a total of four large diameter, FLRFamide-immunopositive axons in this nerve; note that a number of small FLRFamide-immunopositive axons were also present in the *stn*) and bifurcated just anterior to the insertion point of the *acn*s. At the *acn*s, one branch derived from the bifurcation of each axon entered the right *acn* with the other branch of each axon entering the left *acn*. The result of this branching pattern is the four axons seen per *acn* (Fig. 6B).

To confirm the projection pathway of the axons just described, and to attempt to locate the somata of these axons, we conducted a series of experiments in which we backfilled one *acn* with LY and subsequently processed the nerve backfill for FLRFamide immunolabeling (*N*=5 preparations). In these experiments, the backfill site on the *acn* was just distal to the insertion point of this nerve into the *stn*. This location ensured the presence of the FLRFamide-immunopositive axons at the site of nerve transection.

In all backfilled *acn*s, LY-filling was evident in five axons. Four of the five axons were double-labeled by the FLRFamide antibody and could be seen to project into the contralateral *acn* as well as into the *stn*, traveling toward the anterior ganglia (data not shown). At the junction of the *stn* and *son*s, two of the four double-labeled axons entered the right *son* with the remaining pair entering the left *son* (Fig. 10A). Thus, these backfills do confirm the projection pathway of the FLRFamide-containing fibers described above. It should be noted that additional single-labeled FLRFamide immunopostive axons were also present in each *son* (Fig. 10A). These axons too appeared to project into the *stn*. Unlike the double-labeled axons, these FLRFamide immunolabeled fibers bypassed the *acn*s and projected into and innervated the neuropil of the STG (data not shown).

The source of most somata that project from the anterior portion of the STNS to the posterior nerves and STG is the paired CoGs (Coleman et al., 1992). As the CoGs contain numerous FLRFamide-immunopositive cell bodies (approximately 40 somata per ganglion; data not shown), we felt confident that the somata of the FLRFamide axons innervating the ACPs would be found to reside here. While LY routinely reached the CoGs (*N*=8 of 10 CoGs; data not shown), in no preparation were we able to dye-fill any somata in these ganglia. Interestingly, in one CoG, two very weakly dye-filled, FLRFamide-immunopositive axons could be seen to project out of the neuropil toward the *coc*, which connects the STNS to both the supraoesophageal and the fused thoracic ganglia (data not shown). The direction in which these axons projected within the *coc* could not be determined in this ganglion.

The LY-filled *acn* axon not labeled by the FLRFamide antibody also projected into both the contralateral *acn* and the *stn*, but here the fiber traveled posteriorly, toward the STG (Fig. 10B). Though unconfirmed, it appears likely that this fiber is the axon of the anterior median (AM) neuron, a neuron whose soma is located within the STG and is known in numerous decapods to project axons through both *acn*s to innervate the muscles of the cardiac sac region of the foregut (Maynard and Dando, 1974; Selverston and Moulins, 1987; Harris-Warrick et al., 1992).

The FLRFamide-immunopositive axons appear to be the sole source of innervation to the anterior cardiac plexi

As described above, four axons projecting *via* the *son*s and *stn* provide all of the FLRFamide innervation to the ACPs. Moreover, our ultrastructural and LY backfill data suggest that only one other neuron, likely to be the AM neuron, projects through *acn*s, which contain the ACPs. To assess whether the putative AM neuron contributes to the innervation of the

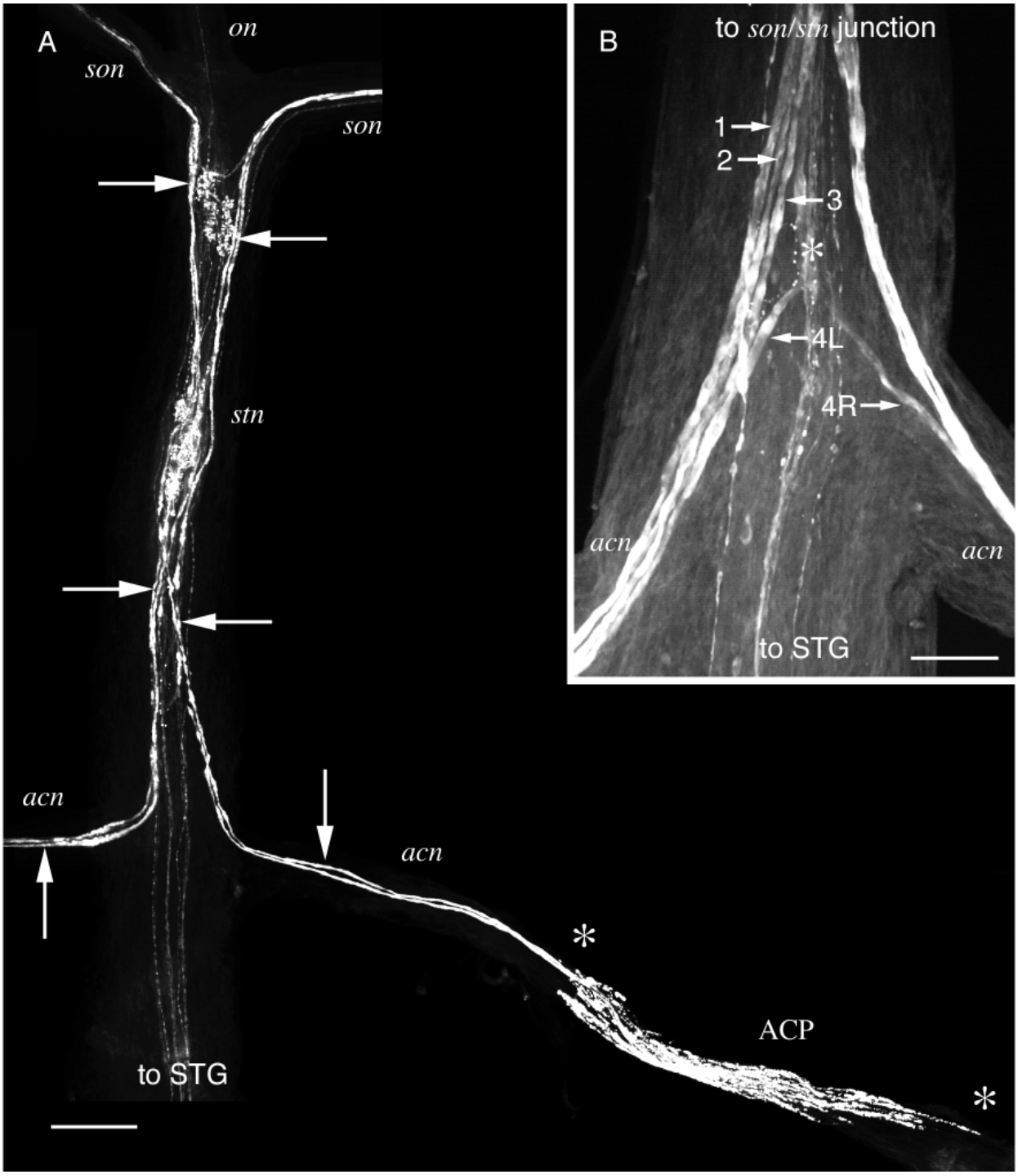

Fig. 6. FLRFamide immunoreactivity in the anterior cardiac plexus (ACP) is derived from four axons which project to the structure through the superior oesophageal (*son*), stomatogastric (*stn*) and anterior cardiac (*acn*) nerves. (A) Montage of seven confocal micrographs showing the projection pathway of the axons that give rise to the ACPs. In this preparation, the axons (denoted by the arrows) travel through much of the nervous system as tightly associated fascicles. These fascicles can be followed unambiguously from the *son*s, through the *stn* and *acn*s to the ACPs. In this image, the beginning and end of the right ACP are defined by asterisks. The left ACP is not shown. In this montage, the individual micrographs are brightest pixel projections of 30–55 optical sections taken at 2.0 μm intervals. (B) Confocal micrograph showing four FLRFamide labeled axons projecting into the *acn*. In this preparation, the four FLRFamide immunopostive axons that arborize into the ACPs are clearly visible entering the left *acn*. Each of these axons (arbitrarily designated 1–4) is indicated with an arrow. The branch point of axon 4 is marked with an asterisk and the left and right projecting branches labeled 4L and 4R, respectively. This image is a brightest pixel projection of 22 optical sections taken at 2.0 μm intervals. Scale bars, 200 μm (A); 100 μm (B). *on*, oesophageal nerve; STG, stomatogastric ganglion.

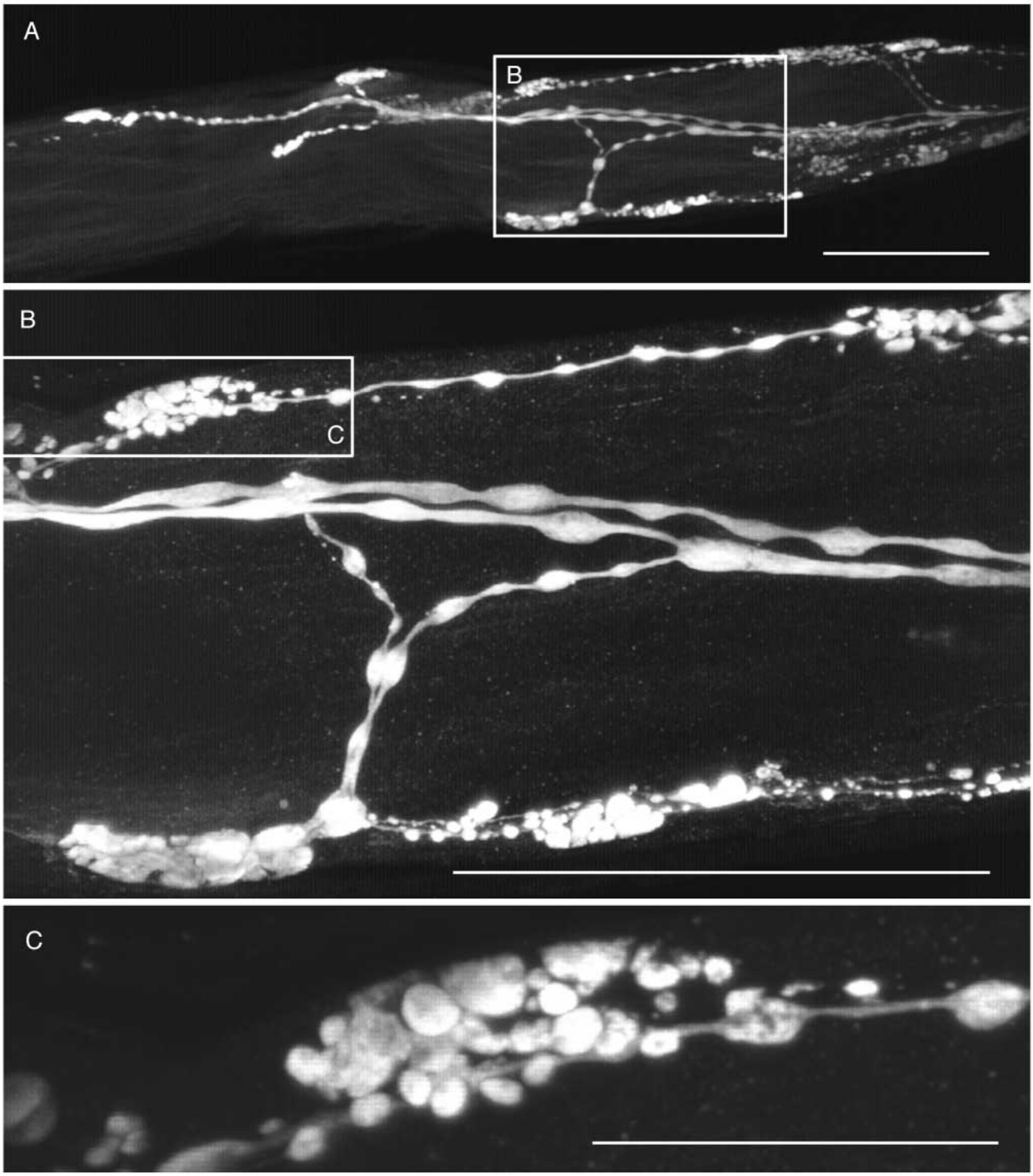

Fig. 7. FLRFamide labeling in the anterior cardiac plexus consists of peripherally located varicosities derived from large diameter fibers. (A) Confocal micrograph showing the distal termination of the left ACP. Here, several immunolabeled fibers can be seen to project fine processes toward the periphery of the anterior cardiac nerve. These fine neurites arborize, producing numerous clusters of varicosities which are located within or just below the *acn* sheath. This image is a brightest pixel projection of 26 optical sections taken at 2.0 μm intervals. (B) A higher magnification view of a portion of the *acn* boxed in A. Note that many of the varicosities are connected together by fine neurites, giving rise to a 'beads on a string'-like conformation. This image is a brightest pixel projection of 24 optical sections taken at 1.0 μm intervals. (C) A further magnified view of one cluster of FLRFamide containing varicosities boxed in B. Note the grape-like cluster of terminal varicosities. This image is a brightest pixel projection of 44 optical sections taken at 0.5 μm intervals. Scale bars, 100 μm (A,B); 25 μm (C).

ACPs, we conducted double-immunolabels of these structures pairing the FLRFamide antibody with an antibody generated against the vesicle-associated protein synapsin. Synapsins are expressed on ELVs and as the AM neuron is known to contain glutamate (contained in ELVs; Selverston and Moulins, 1986), this antibody should be a general marker for its terminals. Since the AM neuron is not FLRFamide immunopositive (no intrinsic STG somata show evidence of FLRFamide labeling in *C. productus*; data not shown), we would expect that if it contributes to the innervation of the ACPs, synapsin-positive, FLRFamide-negative terminals should be present in the double-labeled preparations.

In all double-labeled preparations (*N*=18 ACPs), we found that both the FLRFamide and synapsin immunolabels are coincident in the ACP (Fig. 11). In each ACP, most FLRFamide-immunopositive varicosities were found to exhibit some degree of synapsin labeling. In no ACP did we observe any terminals that contained only synapsin immunoreactivity. Thus, all inputs to the ACPs can be accounted for by the four FLRFamide-immunopositive input axons.

Discussion

The anterior cardiac plexus: an ultrastructurally identifiable neurosecretory site

Regardless of species, or location within the nervous system, crustacean neurosecretory sites possess a highly conserved ultrastructure (Hodge and Chapman, 1958; Fingerman and Aoto, 1959; Knowles, 1965; Bunt and Ashby, 1967; Andrews et al., 1971; Smith, 1974; Silverthorn, 1975; Andrews and Shivers, 1976; Strolenberg et al., 1977; Nordman and Morris, 1980; Weatherby, 1981; Kobierski et al., 1987; Dircksen, 1992; Skiebe et al., 1999; Skiebe and Ganeshina, 2002; Christie et al., 2003). All appear to be separated from the hemolymph space by only an epineurium, often termed the basement membrane or basal lamina. This structure is acellular and appears to be composed of an amorphous, collagen-like material, which is often fenestrated with minute open spaces. Nerve terminals, often in aggregates, lie beneath the epineurium, as do glia and other support cells. The nerve terminals are often densely packed with large, membrane-bound vesicles of varying electron density and, in some neurosecretory sites, small ELVs are also present. The

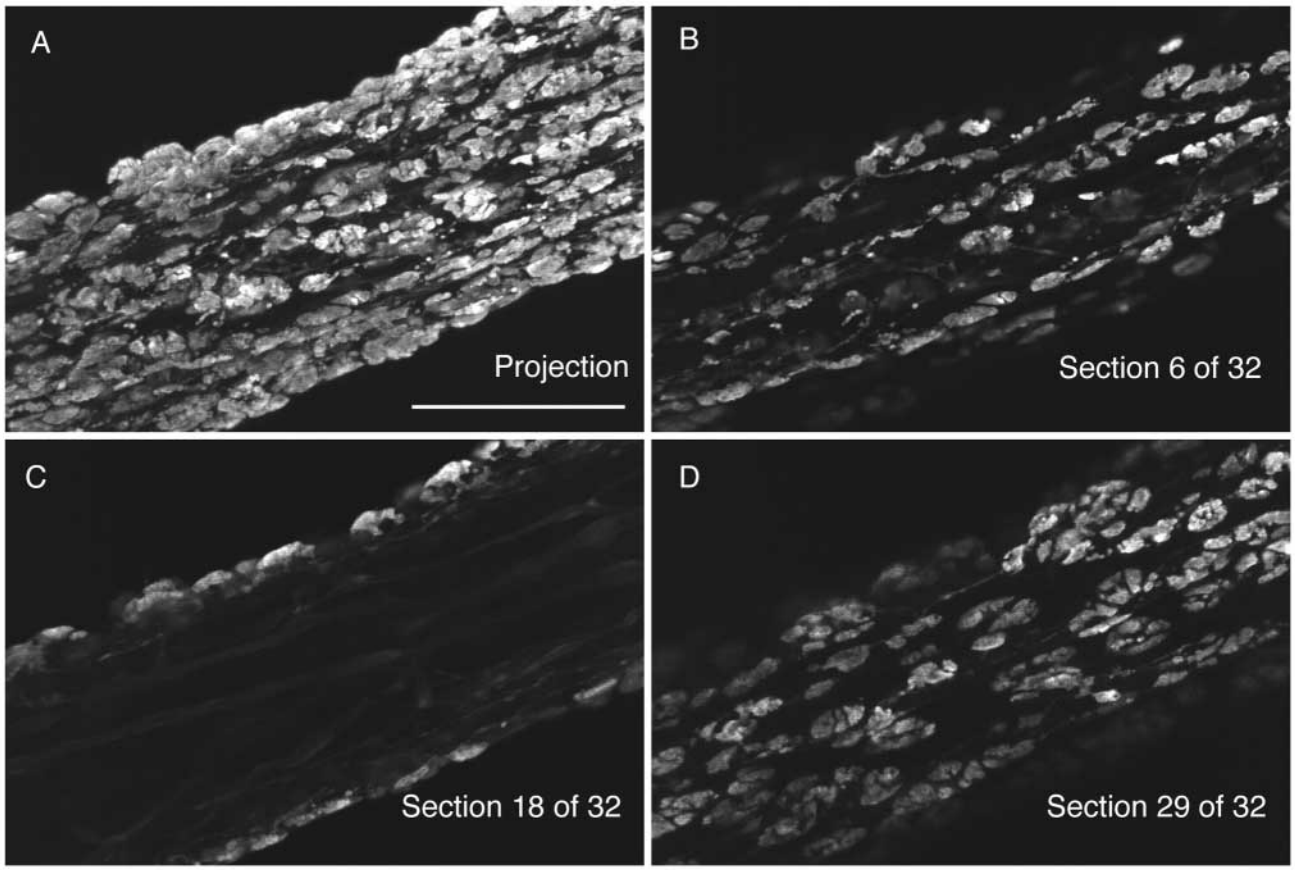

Fig. 8. Clustering of FLRFamide-immunopositive terminals in the anterior cardiac plexus (ACP) often gives rise to a bark-like appearance of this structure. (A) A brightest pixel projection of 32 optical sections taken at 2.0 μm intervals through a portion of the anterior cardiac nerve (*acn*) containing the ACP. (B–D) Single optical sections from the projection shown in A. These images were selected as representative of the labeling seen near the top (B; section 6 of 32), center (C; section 18 of 32) and bottom (D; section 29 of 32) of the *acn*. Note that the FLRFamide immunolabeled terminals that comprise the ACP are concentrated in the peripheral portion of the *acn*, with essentially no terminals present in the core of the nerve. Scale bar, 100 μm.

ACPs of *C. productus* exhibit all of these ultrastructural characteristics; compare Fig. 4 of this study and fig. 1 of Strolenberg et al. (1977), fig. 5 of Weatherby (1981), fig. 8 of Kobierski et al. (1987), fig. 2 of Dircksen (1992) or fig. 10 of Skiebe et al. (1999). As we have shown in this study, each ACP consists of nerve terminals present directly under a well-defined epineurium. The terminals are densely packed with DCVs and also contain a small population of ELVs. Thus, based on ultrastructural morphology, we believe the ACPs are neurosecretory in nature.

In addition to a conserved ultrastructure, many anatomical investigations of crustacean neurosecretory sites show morphological evidence of the exocytosis of DCVs (Bunt and Ashby, 1967; Smith, 1974; Silverthorn, 1975; Andrews and Shivers, 1976; Nordmann and Morris, 1980; Weatherby, 1981; Dircksen, 1992; Christie et al., 2003). As defined by Normann (1969, 1976), an exocytotic event can be seen *via* transmission electron microscopy to consist of several steps: (1) a slight invagination of the plasma membrane of a nerve terminal towards a DCV, (2) direct contact, or docking, of the DCV membrane with the plasma membrane of the terminal, (3) fusion of the terminal and the DCV membranes resulting in the formation of an Ω-figure and (4) extrusion of the electron-dense vesicle core. In our study we have shown that these same exocytotic steps can be seen in transmission electron micrographs of the *C. productus* ACPs (compare Fig. 5 of this study and fig. 11 of Weatherby, 1981). While generally considered a rare occurrence (Strolenberg et al., 1977), we found Ω-figures common on the nerve terminals that comprise the ACPs. In fact, on many terminals, multiple Ω-figures were evident (Figs 4B, 5). The presence of these morphological correlates of neurosecretion further strengthens our belief that the ACPs of *C. productus* are active neuroendocrine signalling centers.

Source of innervation and hormone complement of the anterior cardiac plexi

Nerve backfilling, in combination with light and transmission electron microscopy, shows that all innervation to the ACPs is provided by four axons, which project to these structures *via* the *son*s and *stn*. These axons terminate in the ACPs and do not innervate the muscles of the cardiac sac region of the foregut as does the other axon (presumably that of the AM neuron) present in each *acn*. Our goal with the nerve backfills was to identify the location of the somata innervating the ACPs. While our LY backfills routinely traveled to each of the paired CoGs, which are the source of most of the somata projecting to the posterior portion of the STNS (Coleman et al., 1992) and the location of approximately 40 FLRFamide-immunopositive somata (A. E. Christie, unpublished

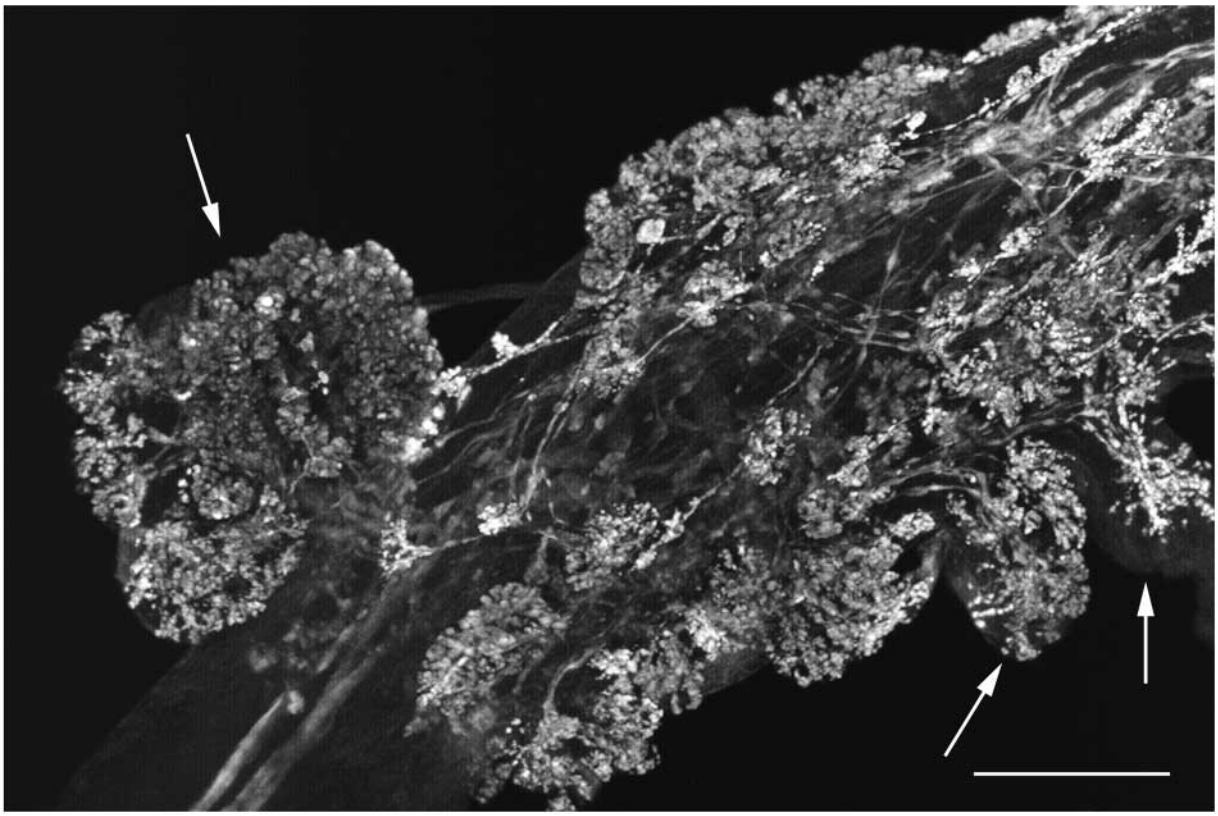

Fig. 9. On some anterior cardiac plexi (ACPs), blister-like protuberances are evident. In some preparations, the ACPs contain multiple blister-like protuberances of the sheath that are densely packed with FLRFamide-immunopositive profiles. In this example, numerous protuberances are present, several of which are indicated with arrows. This image is a brightest pixel projection of 36 optical sections taken at 2.0 μm intervals. Scale bar, 100 μm.

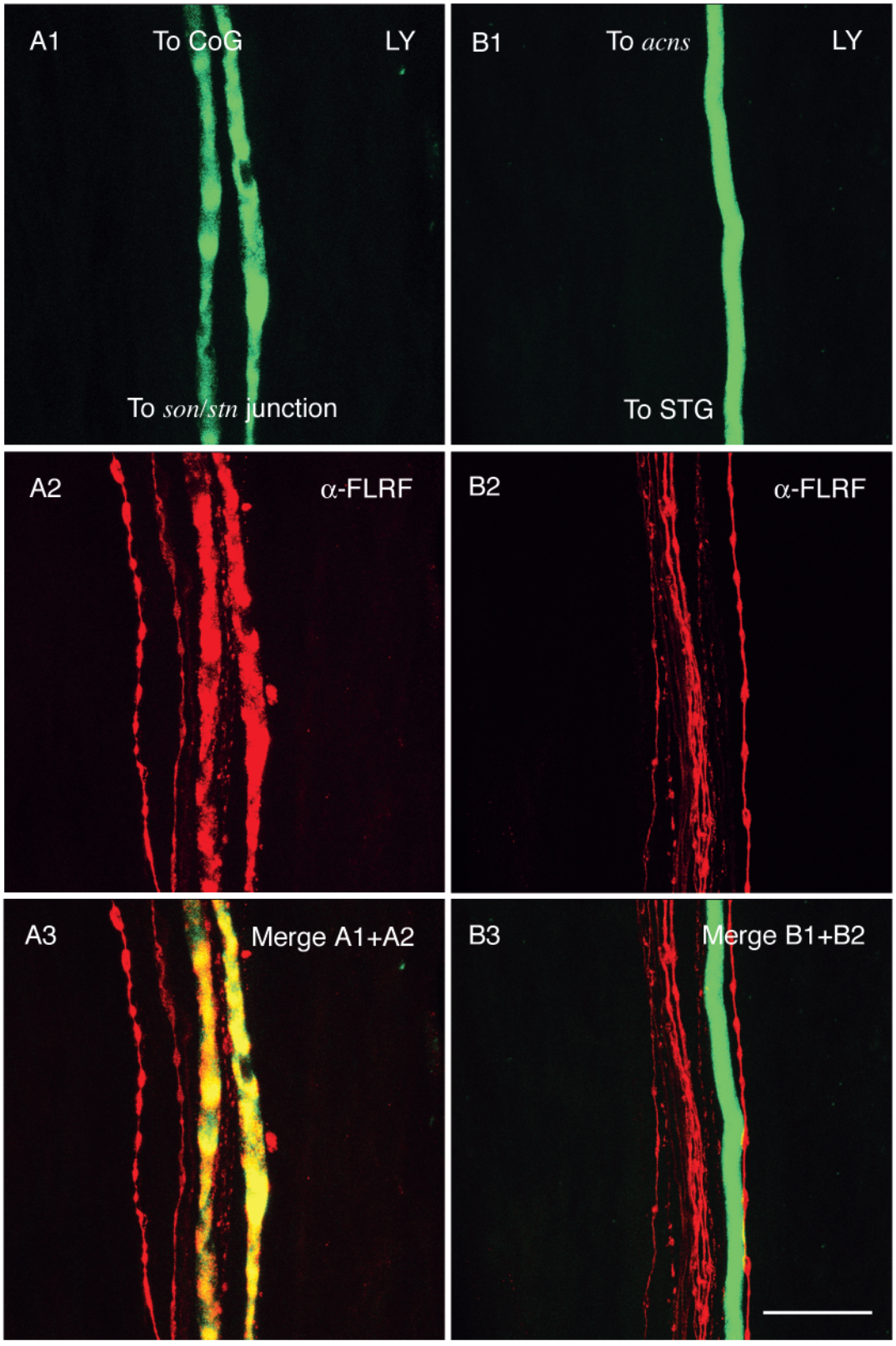

observations), they failed to fill any cell bodies in these ganglia. Thus, it appears possible that the somata responsible for the innervation of the ACPs may reside outside the STNS. In support of this hypothesis is one double-labeled CoG. In this ganglion, weakly dye-filled, FLRFamide-immunopositive axons appeared to project from the CoG neuropil toward the *coc*. Since this nerve connects the CoG with both the supraoesophageal ganglion and the fused thoracic ganglia, both

Fig. 10. Lucifer Yellow-CH dye (LY) backfill of an anterior cardiac nerve (*acn*) produces dye-filling in axons that project posteriorly from the superior oesophageal nerves (*son*s) and anteriorly from the stomatogastric ganglion (STG). (A1–3) LY backfilling of single *acn*s produces dye-filling in two large diameter axons in each of the paired *son*s. These axons are FLRFamide immunopositive. Several smaller diameter FLRFamide-immunopositive axons are also present in each *son*. (B1–3) LY backfilling of single *acn*s also produces dye-filling in a single large diameter axon that projects *via* the stomatogastric nerve (*stn*) from the STG. This axon is not FLRFamide immunopositive. As is seen in the *son*, several small FLRFamide-immunopositive axons are present in the *stn*. (A1–3) Brightest pixel projections of 19 optical sections taken at 1.0 μm intervals through the *son*. (A1) LY dye-filled axons pseudocolored green. (A2) FLRFamide immunoreactivity pseudocolored red. The optical sections used to produce A1 and A2 were simultaneously collected from the same focal planes. (A3) A merged image of A1 and A2. Profiles exhibiting only LY dye-filling or FLRFamide immunolabeling, appear green or red, respectively. Structures showing colocalization of LY dye and FLRFamide label appear yellow (or shades thereof). (B1–3) Brightest pixel projection of 22 optical sections taken at 1.0 μm intervals through the *stn*. Organization and pseudocoloring of B1–3 is identical to that of A1–3. A and B are from the same preparation. Scale bar, 50 μm

are potential locations for the cell bodies innervating the ACPs. At present, we are conducting cobalt chloride backfills from the *acn*s to these ganglia in an attempt to determine if somata in one or both of these sites are the source of the axons innervating the ACPs.

Our ultrastructural analysis of the ACPs shows that these neurohemal release sites contain both DCVs and ELVs. This finding suggests that the structures could contain a diverse complement of hormonal modulators including peptides, amines and classical small molecule transmitters. In this paper, we have used immunocytochemistry to show that each of the four axons that innervate the ACPs exhibit FLRFamide-related staining. We are continuing to survey the ACPs for additional modulators and as this study continues, it will be interesting to see what hormone complement is present at these sites and if the neurons that innervate the plexi have conserved or distinct cotransmitter phenotypes.

Structures homologous to the anterior cardiac plexi are likely present in other Brachyuran species

In decapod crustaceans, some neurosecretory organs appear conserved across phylogeny. In all species thus far examined, structures homologous to the SGs and the POs have been identified (Cooke and Sullivan, 1982). While little work has been done on the PCOs, it appears that these structures are lacking in some species (Cooke and Sullivan, 1982). Whether structures homologous to the ACPs are present in other crabs remains to be determined. There is preliminary evidence that in the genus *Cancer*, the physical structure of the ACPs is conserved. Skiebe and Wollenschläger (2002), using antibodies to vesicle-associated proteins, have shown that structures, apparently homologous to the ACPs, are present on the *acn*s of *C. pagurus*. Likewise, using incident light microscopy, we found iridescent regions on the *acn*s of *Cancer antennarius*, *Cancer anthonyi*, *Cancer borealis*, *Cancer irroratus* and *Cancer magister* (Christie et al., 2002). In these latter species, antibodies to the same vesicle-associated proteins used by Skiebe and Wollenschläger (2002) label the iridescent sites. Moreover, this labeling is identical to the vesicle-associated protein staining seen in the ACPs of *C. productus* (A. E. Christie, unpublished observations). At present, we are conducting transmission electron microscopy on the putative ACPs of these *Cancer* species to confirm that the ultrastructure of these sites is consistent with that of a neuroendocrine release zone.

In addition to crabs of the genus *Cancer*, there is also evidence suggesting that ACP-like structures are present in species from other Brachyuran genera. In their treatise on the organization of the stomatogastric neuromuscular system, Maynard and Dando (1974) reported the presence of an opaque bluish-white region on each *acn* of the blue crab *Callinectes sapidus*. While no detailed description of the site was undertaken, the location of this opaque area is the same as that of the ACP we report here for *C. productus*. We have recently begun an incident light examination of species from a number of other Brachyuran genera (including *Callinectes*, *Carcinus*, *Chionoecetes* and *Telmessus*) and have found iridescent areas on the *acn*s of these animals as well (A. E. Christie and J. M. Edwards, unpublished observations). As more data are collected, it will be interesting to see how broadly conserved ACP-like structures are in Brachyuran species.

It is unclear whether the ACPs, at least as they appear in *C. productus*, will be found in the non-Brachyuran decapods, e.g. Palinura (spiny lobsters) and Astacidea (chelate lobsters and freshwater crayfish). This is due to the fact that the location and branching structure of the *acn*s vary between Brachyurans and these other animals (Maynard and Dando, 1974). In their extensive descriptions of the STNS of both the Caribbean spiny lobster *Panulirus argus* and the American lobster *H. americanus*, Maynard and Dando (1974) make no mention of a putative neurosecretory site on nerves considered homologous to the crab *acn*s. Likewise, vesicle-associated protein labeling in several Palinuran and Astacidean species shows no evidence of immunopositive plexi on the *acn* homologs (Skiebe, 2000; Skiebe and Ganeshina, 2000; Skiebe and Wollenschläger, 2002).

It is interesting to note that in *H. americanus*, as well as in the California spiny lobster *P. interruptus* and the Australian freshwater crayfish *C. destructor* and *C. quadricarinatus*, there is evidence of a collection of neurosecretory profiles in the nerves of the anterior portion of the STNS (Kobierski et al., 1987; Kilman and Marder, 1996; Kilman, 1998; Skiebe, 2000; Skiebe and Ganeshina, 2000; Skiebe and Wollenschläger, 2002; Christie et al., 2003). In these animals, this neurosecretory region overlies the same general region of the foregut as the portion of the *acn* containing the ACP. Transmission electron microscopy shows that in these species the sheath of nerves in the anterior portion of the STNS is

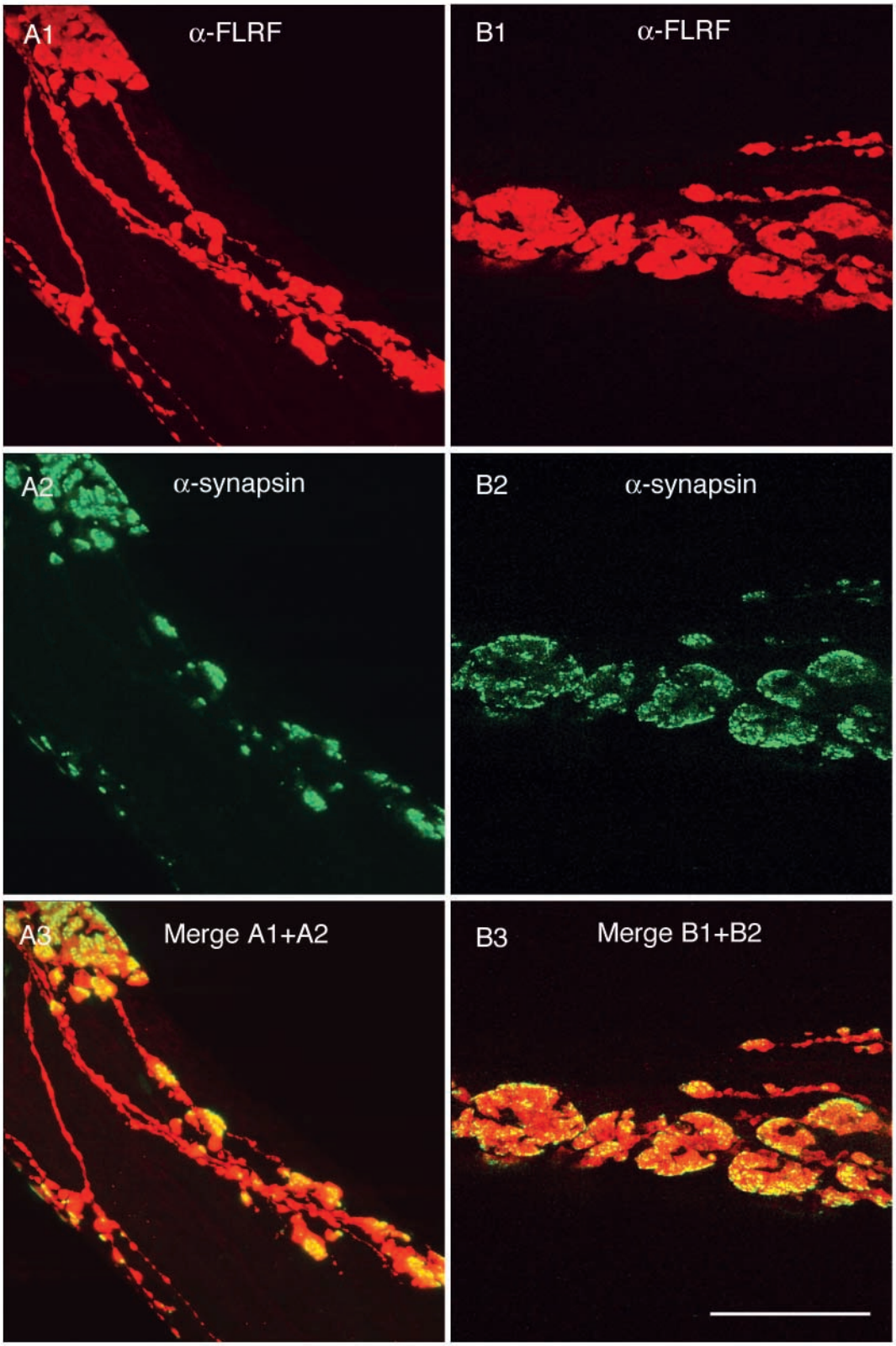

replete with neurosecretory-type profiles that are similar in their ultrastructure to those found in the ACPs of *C. productus* (Kobierski et al., 1987; Kilman, 1998; Skiebe, 2000; Skiebe and Ganeshina, 2000, Skiebe and Wollenschläger, 2002; Christie et al., 2003). Whether this site is the Astacidean and Palinuran homolog of the Brachyuran ACPs remains unclear. The common ultrastructure of the sites and their general location within the STNS suggest this

Fig. 11. Synapsin-like labeling is restricted to FLRFamide-immunopositive terminals in the anterior cardiac plexus (ACP). Five axons are present in the portion of the anterior cardiac nerve containing the ACP. Four of the five axons are FLRFamide immunopositive and contribute innervation to the ACP. To assess whether the remaining axon contributes to the innervation of the ACPs, double-immunolabels pairing FLRFamide and synapsin antibodies were conducted. In all preparations, the synapsin label was found localized in FLRFamide-immunopositive terminals. Most FLRFamide labeled terminals exhibited some degree of synapsin staining. In no preparation were any terminals found that contained only synapsin immunoreactivity. Interestingly, within a given terminal, the FLRFamide and synapsin labels are often non-uniformly segregated. (A1–3) and (B1–3) show examples of this localization from two different preparations. (A1–3) Brightest pixel projections of 19 optical sections taken at 1.0 μm intervals. (A1) FLRFamide immunoreactivity pseudocolored red. (A2) Synapsin immunoreactivity pseudocolored green. The optical sections used to produce A1 and A2 were simultaneously collected from the same focal planes. (A3) A merged image of A1 and A2. Profiles exhibiting only FLRFamide or synapsin immunolabeling appear red or green, respectively. Structures showing coincidence of FLRFamide and synapsin labels appear yellow (or shades thereof). (B1–3) Brightest pixel projection of 12 optical sections taken at 1.0 μm intervals. Organization and pseudocoloring of B1–3 is identical to that of A1–3. Scale bar, 50 μm.

may be the case. Recently, however, we have found that the source of innervation to the respective sites is not conserved. As we show in this paper, the ACPs are innervated by only four axons. Our backfilling experiments suggest that the CoGs are not the location of the somata of these fibers. In the freshwater crayfish, *C. quadricarinatus*, we have found that at least 24 CoG neurons do contribute to the innervation of the plexus (Christie et al., 2003). The likely differing locations of the somata innervating the *C. productus* ACPs *versus* the *C. quadricarinatus* plexus suggest that the neurons projecting to the two sites could receive different synaptic input resulting in quite different secretory output. Clearly additional study will be needed to determine the degree of homology between the Brachuran and the Astacidean and Palinuran plexi.

Physiological functions of the anterior cardiac plexi

While the physiological role(s) of the ACPs within the STNS remains unknown, several functions have been generally ascribed to circulating hormones in this system. Many substances have been demonstrated to have neuromodulatory capabilities in the STNS. The effects of many of these modulators have been shown to be highly concentration dependent, particularly on the circuits contained within the STG. It has been shown recently that the majority of neuroactive substances that modulate the STG circuits likely do so both *via* intrinsic release and through the hemolymph (Christie et al., 1995; Skiebe, 2001). This dual function has significant physiological consequences, as the concentration of a modulator resulting from synaptic/local *versus* neuroendocrine release is likely to be quite different at any given target neuron (Keller, 1992; Marder et al., 1995; Christie et al., 1995). Thus, it is likely that hormonal delivery of a modulator will produce quantitatively and/or qualitatively different effects from those that occur when the same substance is locally released within the ganglion.

In this paper, we demonstrate that the ACPs of *C. productus* exhibit FLRFamide immunoreactivity. In this species, FLRFamide immunolabeling is also present in the neuropil of STG (A. E. Christie, unpublished observations). While the effects of FLRFamide-related peptides on the STG circuit have not been determined in *C. productus*, in a related crab these peptides have been shown to be potent modulators of the neural circuits contained here (Weimann et al., 1993). In *C. borealis*, the threshold for FLRFamide action on the STG is quite low (10^{-11} to 10^{-10} mol l^{-1}), well within the realm that could result from hormonal release (Weimann et al., 1993). At these low concentrations, only the pyloric circuit is activated or enhanced. At higher concentrations (10^{-7} mol l^{-1}), which almost certainly requires intrinsic release within the STG neuropil, both the pyloric and gastric mill circuits are activated/enhanced (Weimann et al., 1993). Thus, in *C. borealis*, it is likely that hormonal delivery of FLRFamide elicits qualitatively distinct effects from those that are produced by intrinsic release of this peptide within the ganglion. Given the multiple tissue localizations of FLRFamide in *C. productus*, a similar effect is expected.

Neural circuits are not the only targets of circulating hormones in the stomatogastric neuromuscular system. Several studies have demonstrated that the muscles of the foregut are also influenced by circulating substances, including FLRFamide-related peptides. In the foregut of *C. borealis*, many muscles that lack direct innervation by a given neuroactive compound are nonetheless modulated by that substance (Jorge-Rivera and Marder, 1996, 1997; Jorge-Rivera, 1997; Jorge-Rivera et al., 1998). In *C. borealis*, 15 out of 17 stomatogastric muscles tested were found to be modulated by extended FLRFamide peptides (Jorge-Rivera and Marder, 1996). This modulation has been shown to include induction of long-lasting myogenic activity, as well as increased amplitude of nerve-evoked contractions, excitatory junctional potentials and excitatory junctional currents (Jorge-Rivera and Marder, 1996). The threshold concentration for these actions was determined to be in the range of 10^{-10} mol l^{-1}, which is clearly within the concentration range expected of a circulating hormone (Jorge-Rivera and Marder, 1996). It has been postulated that hormonally delivered FLRFamide-related peptides are crucial for maintaining appreciable muscle contractions in response to the low-frequency and low-intensity motor discharge that drives many muscles in this system (Jorge-Rivera and Marder, 1996). The same muscles that were shown to be sensitive to FLRFamide in *C. borealis* also exist in *C. productus*. We have found that, here too, they lack direct innervation by FLRFamide containing axons (A. E. Christie, unpublished observations). If

they are also modulated by FLRFamide, then the ACPs may well be a source of this modulatory control.

Finally, it is possible that agents released from the ACPs exert influence on target tissues far beyond the stomatogastric neuromuscular system. Studies in crustaceans have shown that many substances released into the circulatory system influence target tissues distant from their point of release. Hormonally released FLRFamides have been shown to affect a number of target tissues in crustaceans (Trimmer et al., 1987; Krajniak, 1991; Keller, 1992; McGaw and McMahon, 1995; Worden et al., 1995). Several studies have shown that these peptides have potent effects on the heart (Trimmer et al., 1987; Krajniak, 1991; Keller, 1992; McGaw and McMahon, 1995). FLRFamide peptides have also been shown to affect the contractile properties of the hindgut (Keller, 1992). As future studies focus on the physiological role of the ACPs in crabs, it will be interesting to see how far-reaching the actions of these neuroendocrine structures may be.

We would like to thank Drs E. Buchner (Universität Würzburg, Würzburg, Germany) and M. Nusbaum (University of Pennsylvania, Philadelphia, Pennsylvania, USA) for their gifts of the synapsin antibody and *Cancer borealis* tachykinin-related peptide Ia, respectively. We thank Dr B. Swalla (University of Washington, Seattle, Washington, USA) for the use of her Nikon epiflourescense microscope and CoolSNAP camera system. We also thank Electron Microscopy Sciences, Jackson ImmunoResearch Laboratories, Peninsula Laboratories and Vector Laboratories Inc. for contributing reagents used in the portion of this study conducted during a Spring 2002 Research Apprenticeship Class at Friday Harbor Laboratories. Finally we thank Dr D. Baldwin, Ms L. Baldwin, Ms C. Ngo and Dr D. Prince for reading and commenting on early versions of this manuscript. This work was supported by NINDS (NS15697), the University of Washington, the Mary Gates Endowment for Students and the Washington Research Foundation. Collection of some of the animals used in this study was done under the auspices of Washington Department of Fish and Wildlife Scientific Collection Permit #03-018a.

References

Alexandrowicz, J. S. and Carlisle, D. B. (1953). Some experiments on the function of the pericardial organs in Crustacea. *J. Mar. Biol. Assn. UK* **32**, 175-192.

Andrews, P. M., Copeland, D. E. and Fingerman, M. (1971). Ultrastructural study of the neurosecretory granules in the sinus gland of the blue crab, *Callinectes sapidus*. *Z. Zellforsch.* **113**, 461-471.

Andrews, R. D. and Shivers, R. R. (1976). Ultrastructure of neurosecretory granule exocytosis by crayfish sinus gland induced with ionic manipulations. *J. Morphol.* **150**, 253-278.

Beltz, B. S. and Kravitz, E. A. (1983). Mapping of serotonin-like immunoreactivity in the lobster nervous system. *J. Neurosci.* **3**, 585-602.

Bliss, D. E. (1951). Metabolic effects of sinus gland or eyestalk removal in the land crab, *Gecarcinus lateralis*. *Anat. Rec.* **111**, 502-503.

Blitz, D. M., Christie, A. E., Coleman, M. J., Norris, B. J., Marder, E. and Nusbaum, M. P. (1999). Different proctolin neurons elicit distinct motor patterns from a multifunctional neuronal network. *J. Neurosci.* **19**, 5449-5463.

Bunt, A. and Ashby, E. A. (1967). Ultrastructure of the sinus gland of the crayfish *Procambarus clarkii*. *Gen. Comp. Endocrol.* **9**, 334-342.

Carlisle, D. B. and Knowles, F. G. (1959). *Endocrine Control in Crustacea*. London: Cambridge University Press.

Chang, E. S. (1993). Comparative endocrinology of molting and reproduction: insects and crustaceans. *Annu. Rev. Entomol.* **38**, 161-180.

Chang, E. S., Chang, S. A., Beltz, B. S. and Kravitz, E. A. (1999). Crustacean hyperglycemic hormone in the lobster nervous system: localization and release from cells in the subesophageal ganglion and thoracic second roots. *J. Comp. Neurol.* **414**, 50-56.

Christie, A. E., Baldwin, D. H., Marder, E. and Graubard, K. (1997b). Organization of the stomatogastric neuropil of the crab, *Cancer borealis*, as revealed by modulator immunocytochemistry. *Cell Tiss. Res.* **288**, 135-148.

Christie, A. E., Edwards, J. M., Cherny, E., Clason, T. A. and Graubard, K. (2003). Immunocytochemical evidence for nitric oxide- and carbon monoxide-producing neurons in the stomatogastric nervous system of the crayfish, *Cherax quadricarinatus*. *J. Comp. Neurol.* **467**, 293-306.

Christie, A. E., Graubard, K., Cain, S. D., Chernichenko, E., Clason, T. A., Cowan, N. G., Edwards, J. M., Lin, M., Manhas, A. S., Nold, K. A., Sellereit, K. L. and Strassburg, H.-P. (2002). Intrinsic neurosecretory organs within the crab stomatogastric nervous system. Program No. 2070.21. 2002 Abstract Viewer/Itinerary Planner. Washington, DC: Society for Neuroscience, 2002. Online.

Christie, A. E., Lundquist, C. T., Nassel, D. R. and Nusbaum, M. P. (1997a). Two novel tachykinin-related peptides from the nervous system of the crab *Cancer borealis*. *J. Exp. Biol.* **200**, 2279-2294.

Christie, A. E. and Nusbaum, M. P. (1995). Distribution and effects of corazonin-like and allatotropin-like peptides in the crab stomatogastric nervous system. *Soc. Neurosci. Abstr.* **21**, 629.

Christie, A. E. and Nusbaum, M. P. (1998). Neuroendocrine influence on local modulatory actions in the crab stomatogastric ganglion. *Soc. Neurosci. Abstr.* **24**, 1895.

Christie, A. E., Skiebe, P. and Marder, E. (1995). Matrix of neuromodulators in neurosecretory structures of the crab *Cancer borealis*. *J. Exp. Biol.* **198**, 2431-2439.

Chung, J. S., Dircksen, H. and Webster, S. G. (1999). A remarkable, precisely timed release of hyperglycemic hormone from endocrine cells in the gut is associated with ecdysis in the crab *Carcinus maenas*. *Proc. Natl. Acad. Sci. USA* **96**, 13103-13107.

Coleman, M. J., Nusbaum, M. P., Cournil, I. and Claiborne, B. J. (1992). Distribution of modulatory inputs to the stomatogastric ganglion of the crab, *Cancer borealis*. *J. Comp. Neurol.* **325**, 581-594.

Cooke, I. M. and Sullivan, R. E. (1982). Hormones and neurosecretion. In *The Biology Of Crustacea*, vol. 3, *Neurobiology: Structure and Function* (ed. H. L. Atwood and D. C. Sandeman), pp. 206-278. New York: Academic Press.

Dircksen, H. (1992). Fine structure of the neurohemal sinus gland of the shore crab, *Carcinus maenas*, and immuno-electron-microscopic identification of neurosecretory endings according to their neuropeptide contents. *Cell Tiss. Res.* **269**, 249-266.

Evans, P. D., Kravitz, E. A., Talamo, B. R. and Wallace, B. G. (1976). The association of octopamine with specific neurones along lobster nerve trunks. *J. Physiol.* **262**, 51-70.

Fénelon, V. S., Casasnovas, B., Faumont, S. and Meyrand, P. (1998). Ontogenetic alteration in peptidergic expression within a stable neuronal population in lobster stomatogastric nervous system. *J. Comp. Neurol.* **399**, 289-305.

Fingerman, M. (1997). Crustacean endocrinology: a retrospective, prospective, and introspective analysis. *Physiol. Zool.* **70**, 257-269.

Fingerman, M. and Aoto, T. (1959). The neurosecretory system of the dwarf crayfish, *Cambarellus schefeldti*, as revealed by light and electron microscopy. *Trans. Am. Microsc. Soc.* **78**, 305-317.

Fingerman, M., Jackson, N. C. and Nagabhushanam, R. (1998). Hormonally-regulated functions in crustaceans as biomarkers of environmental pollution. *Comp. Biochem. Physiol.* **120C**, 343-350.

Friend, B. J. (1976). Morphology and location of dense-core vesicles in the stomatogastric ganglion of the lobster, *Panulirus interruptus*. *Cell Tiss. Res.* **175**, 369-390.

Harris-Warrick, R. M., Marder, E., Selverston, A. I. and Moulins, M. (ed.) (1992). *Dynamic Biological Networks: The Stomatogastric Nervous System.* Cambridge: MIT Press.

Heinzel, H. G., Weimann, J. M. and Marder, E. (1993). The behavioral repertoire of the gastric mill in the crab, *Cancer pagurus*: an in situ

endoscopic and electrophysiological examination. *J. Neurosci.* **13**, 1793-1803.

Hodge, M. H. and Chapman, G. B. (1958). Some observations on the fine structure of the sinus gland of a land crab, *Gecarcinus lateralis*. *J. Biophys. Biochem. Cytol.* **4**, 571-574.

Huberman, A. (1990). Hormonal control of molting in crustaceans. *Prog. Clin. Biol. Res.* **342**, 205-210.

Jorge-Rivera, J. C. (1997). Modulation of stomatogastric musculature in the crab, *Cancer borealis*. PhD dissertation, Brandeis University, Waltham USA.

Jorge-Rivera, J. C. and Marder, E. (1996). TNRNFLRFamide and SDRNFLRFamide modulate muscles of the stomatogastric system of the crab *Cancer borealis*. *J. Comp. Physiol.* **179A**, 741-751.

Jorge-Rivera, J. C. and Marder, E. (1997). Allatostatin decreases stomatogastric neuromuscular transmission in the crab *Cancer borealis*. *J. Exp. Biol.* **200**, 2937-2946.

Jorge-Rivera, J. C., Sen, K., Birmingham, J. T., Abbott, L. F. and Marder, E. (1998). Temporal dynamics of convergent modulation at a crustacean neuromuscular junction. *J. Neurophysiol.* **80**, 2559-2570.

Keller, R. (1992). Crustacean neuropeptides: structures, functions and comparative aspects. *Experientia* **48**, 439-448.

Kilman V. L. (1998). Multiple roles of neuromodulators throughout life: a anatomical study of the crustacean stomatogastric nervous system. PhD dissertation, Brandeis University, Waltham, USA.

Kilman, V., Fenelon, V. S., Richards, K. S., Thirumalai, V., Meyrand, P. and Marder, E. (1999). Sequential developmental acquisition of cotransmitters in identified sensory neurons of the stomatogastric nervous system of the lobsters, *Homarus americanus* and *Homarus gammarus*. *J. Comp. Neurol.* **408**, 318-334.

Kilman, V. L. and Marder E. (1996). Ultrastructure of the stomatogastric ganglion neuropil of the crab, *Cancer borealis*. *J. Comp. Neurol.* **374**, 362-375.

King, D. G. (1976). Organization of crustacean neuropil. I. Patterns of synaptic connections in lobster stomatogastric ganglion. *J. Neurocytol.* **5**, 207-237.

Klagges, B. R. E., Heimbeck, G., Godenschwege, T. A., Hofbauer, A., Pflugfelder, G. O., Reifegerste, R., Reisch, D., Schaupp, M., Buchner, S. and Buchner, E. (1996). Invertebrate synapsins: a single gene codes for several isoforms in *Drosophila*. *J. Neurosci.* **15**, 3154-3165.

Knowles, F. G. W. (1965). Neuroendocrine correlations at the level of ultrastructure. *Arch. Anat. Microsc. Morph. Exp.* **54**, 343-358.

Kobierski, L. A., Beltz, B. S., Trimmer, B. A. and Kravitz, E. A. (1987). FMRFamide-like peptides of *Homarus americanus*: distribution, immunocytochemical mapping, and ultrastructural localization in terminal varicosities. *J. Comp. Neurol.* **266**, 1-15.

Krajniak, K. G. (1991). The identification and structure-activity relations of a cardioactive FMRFamide-related peptide from the blue crab *Callinectes sapidus*. *Peptides* **12**, 1295-1302.

Lee, C. Y., Zou, H. S., Yau, S. M., Ju, Y. R. and Liau, C. S. (2000). Nitric oxide synthase activity and immunoreactivity in the crayfish *Procambarus clarkii*. *Neurorep.* **11**, 1273-1276.

Livingstone, M. S., Schaeffer, S. F. and Kravitz, E. A. (1981). Biochemistry and ultrastructure of serotonergic nerve endings in the lobster: serotonin and octopamine are contained in different nerve endings. *J. Neurobiol.* **12**, 27-54.

Marder, E. and Calabrese, R. L. (1996). Principles of rhythmic motor pattern generation. *Physiol. Rev.* **76**, 687-717.

Marder, E., Christie, A. E. and Kilman, V. L. (1995). Functional organization of cotransmission systems: lessons from small nervous systems. *Invert Neurosci.* **1**, 105-112.

Marder, E., Hooper, S. L. and Siwicki, K. K. (1986). Modulatory action and distribution of the neuropeptide proctolin in the crustacean stomatogastric nervous system. *J. Comp. Neurol.* **243**, 454-467.

Marder, E., Jorge-Rivera, J. C., Kilman, V. and Weimann, J. M. (1997). Peptidergic modulation of synaptic transmission in a rhythmic motor system. In *The Synapse: In Development, Health and Disease*, vol 2 (ed. B. W. Festoff, D. Hantaï and B. A. Citron), pp. 213-233. Greenwhich, CT: JAI Press Inc.

Marder, E., Skiebe, P. and Christie, A. E. (1994). Multiple modes of network modulation. *Verh. Dtsch. Zool. Ges.* **87**, 177-184.

Maynard, D. M. (1961a). Thoracic neurosecretory structures in Brachyura. I. Gross anatomy. *Biol. Bull.* **121**, 316-329.

Maynard, D. M. (1961b). Thoracic neurosecretory structures in Brachyura. II. Secretory neurons. *Gen. Comp. Endocrinol.* **1**, 237-263.

Maynard, D. M. and Dando, M. R. (1974). The structure of the stomatogastric neuromuscular system in *Callinectes sapidus*, *Homarus americanus* and *Panulirus argus* (Decapoda Crustacea). *Phil. Trans. R. Soc. Lond. B* **268**, 161-220.

Maynard, D. M. and Maynard, E. (1962). Thoracic neurosecretory structures in Brachyura. III. Microanatomy of peripheral structures. *Gen. Comp. Endocrinol.* **2**, 12-28.

McGaw, I. J. and McMahon, B. R. (1995). The FMRFamide-related peptides F1 and F2 alter hemolymph distribution and cardiac output in the crab *Cancer magister*. *Biol. Bull.* **188**, 186-196.

Mercier, A. J., Orchard, I., TeBrugge, V. and Skerrett, M. (1993). Isolation of two FMRFamide-related peptides from crayfish pericardial organs. *Peptides* **14**, 137-143.

Meyrand, P., Faumont, S., Simmers, J., Christie, A. E. and Nusbaum, M. P. (2000). Species-specific modulation of pattern-generating circuits. *Eur. J. Neurosci.* **12**, 2585-2596.

Nordmann, J. J. and Morris, J. F. (1980). Depletion of neurosecretory granules and membrane retrieval in the sinus gland of the crab. *Cell Tiss. Res.* **205**, 31-42.

Normann, T. C. (1969). Experimentally induced exocytosis of neurosecretory granules. *Exp. Cell Res.* **55**, 285-287.

Normann, T. C. (1976). Neurosecretion by exocytosis. *Int. Rev. Cytol.* **46**, 1-77.

Passano, L. M. (1951). The X-organ-sinus gland system in crabs. *Anat. Rec.* **111**, 502.

Phlippen, M. K., Webster, S. G., Chung, J. S. and Dircksen, H. (2000). Ecdysis of decapod crustaceans is associated with a dramatic release of crustacean cardioactive peptide into the haemolymph. *J. Exp. Biol.* **203**, 521-536.

Pulver S. R. and Marder, E. (2002). Neuromodulatory complement of the pericardial organs in the embryonic lobster, *Homarus americanus*. *J. Comp. Neurol.* **451**, 79-90.

Rao, K. R. (1992). Crustacean pigment-dispersing hormones: chemistry, distribution and actions. *Pigment Cell Res.* **2**, 266-270.

Rao, K. R. and Riehm, J. P. (1993). Pigment-dispersing hormones. *Ann. NY Acad. Sci. USA* **680**, 78-88.

Reynolds, E. S. (1963). The use of lead citrate at high pH as an electron opaque stain in electron microscopy. *J. Cell Biol.* **17**, 208.

Rodriguez-Sosa, L., Calderon, J., Becerra, E. and Arechiga, H. (1994). Regional distribution and immunocytological localization of red pigment concentrating hormone in the crayfish eyestalk. *Gen. Comp. Endocrinol.* **95**, 443-456.

Schmidt, M. and Ache, B. W. (1994a). FMRFamide-like immunoreactivity in presumptive chemosensory afferents of the spiny lobster, *Panulirus argus*. *Brain Res.* **653**, 315-324.

Schmidt, M. and Ache, B. W. (1994b). Descending neurons with dopamine-like or with substance P/FMRFamide-like immunoreactivity target the somata of olfactory interneurons in the brain of the spiny lobster, *Panulirus argus*. *Cell Tiss. Res.* **278**, 337-352.

Schwarz, T. L., Lee, G. M., Siwicki, K. K., Standaert, D. G. and Kravitz, E. A. (1984). Proctolin in the lobster: the distribution, release, and chemical characterization of a likely neurohormone. *J. Neurosci.* **4**, 1300-1311.

Selverston, A. I. and Moulins, M. (ed.) (1987). *The Crustacean Stomatogastric System.* Berlin: Springer.

Silverthorn, S. U. (1975). Neurosecretion in the sinus gland of the fiddler crab *Uca pugnax*. *Cell Tiss. Res.* **165**, 129-135.

Siwicki, K. K. and Bishop, C. A. (1986). Mapping of proctolin-like immunoreactivity in the nervous systems of lobster and crayfish. *J. Comp. Neurol.* **243**, 435-453.

Siwicki, K. K., Beltz, B. S. and Kravitz, E. A. (1987). Proctolin in identified serotonergic, dopaminergic, and cholinergic neurons in the lobster, *Homarus americanus*. *J. Neurosci.* **7**, 522-532.

Siwicki, K. K., Beltz, B. S., Schwarz, T. L. and Kravitz, E. A. (1985). Proctolin in the lobster nervous system. *Peptides* **3**, 393-402.

Skiebe, P. (2000). A synaptotagmin antibody marks neurohemal release sites in the stomatogastric nervous system (STNS) of a decapod crustacean. *Eur. J. Neurosci.* **12**, 451.

Skiebe, P. (2001). Neuropeptides are ubiquitous chemical mediators: Using the stomatogastric nervous system as a model system. *J. Exp. Biol.* **204**, 2035-2048.

Skiebe, P., Dietel, C. and Schmidt, M. (1999). Immunocytochemical localization of FLRFamide-, proctolin-, and CCAP-like peptides in the stomatogastric nervous system and neurohemal structures of the crayfish, *Cherax destructor*. *J. Comp. Neurol.* **414**, 511-532.

Skiebe, P., Dreger, M., Meseke, M., Evers, J. F. and Hucho, F. (2002). Identification of orcokinins in single neurons in the stomatogastric nervous system of the crayfish, *Cherax destructor*. *J. Comp. Neurol.* **444**, 245-259.

Skiebe, P. and Ganeshina, O. (2000). Synaptic neuropil in nerves of the crustacean stomatogastric nervous system: an immunocytochemical and electron microscopical study. *J. Comp. Neurol.* **420**, 373-397.

Skiebe, P. and Wollenschläger, T. (2002). Putative neurohemal release zones in the stomatogastric nervous system of decapod crustaceans. *J. Comp. Neurol.* **453**, 280-291.

Smith, G. (1974). Ultrastructure of the sinus gland of *Carcinus maenas* (Crustacea: Decapoda). *Cell Tiss. Res.* **155**, 117-125.

Soyez, D. (1997). Occurrence and diversity of neuropeptides from the crustacean hyperglycemic hormone family in arthropods. A short review. *Ann. NY Acad. Sci. USA* **814**, 319-323.

Stangier, J., Dircksen, H. and Keller, R. (1986). Identification and immunocytochemical localization of proctolin in pericardial organs of the shore crab, *Carcinus maenas*. *Peptides* **7**, 67-72.

Stangier, J., Hilbich, C., Dircksen, H. and Keller, R. (1988). Distribution of a novel cardioactive neuropeptide (CCAP) in the nervous system of the shore crab *Carcinus maenas*. *Peptides* **9**, 795-800.

Strolenberg, G. E. C. M., van Helden, H. P. M. and van Herp, F. (1977). The ultrastructure of the sinus gland of the crayfish *Astacus leptodactylus* (Nordmann). *Cell Tiss. Res.* **180**, 203-210.

Sullivan, R. E., Friend, B. J. and Barker, D. L. (1977). Structure and function of spiny lobster ligamental nerve plexuses: evidence for synthesis, storage, and secretion of biogenic amines. *J. Neurobiol.* **8**, 581-605.

Tierney, A. J., Blanck, J. and Mercier, J. (1997). FMRFamide-like peptides in the crayfish (*Procambarus clarkii*) stomatogastric nervous system: Distribution and effects on the pyloric motor pattern. *J. Exp. Biol.* **200**, 3221-3233.

Trimmer, B. A., Kobierski, L. A., Kravitz, E. A. (1987). Purification and characterization of FMRFamidelike immunoreactive substances from the lobster nervous system: isolation and sequence analysis of two closely related peptides. *J. Comp. Neurol.* **266**, 16-26.

Turrigiano, G. G. and Selverston, A. I. (1989). Cholecystokinin-like peptide is a modulator of a crustacean central pattern generator. *J. Neurosci.* **9**, 2486-2501.

Turrigiano, G. G. and Selverston, A. I. (1990). A cholecystokinin-like hormone activates a feeding-related neural circuit in lobster. *Nature* **344**, 866-868.

Wainwright, G., Webster, S. G., Wilkinson, M. C., Chung, J. S. and Rees, H. H. (1996). Structure and significance of mandibular organ-inhibiting hormone in the crab, *Cancer pagurus*. Involvement in multihormonal regulation of growth and reproduction. *J. Biol. Chem.* **271**, 12749-12754.

Wang, Y. J., Hayes, T. K., Holman, G. M., Chavez, A. R. and Keeley, L. L. (2000). Primary structure of CHH/MIH/GIH-like peptides in sinus gland extracts from *Penaeus vannamei*. *Peptides* **21**, 477-484.

Weatherby, T. M. (1981). Ultrastructural study of the sinus gland of the crab, *Cardisoma carnifex*. *Cell Tiss. Res.* **220**, 293-312.

Webster, S. G., Dircksen, H. and Chung, J. S. (2000). Endocrine cells in the gut of the shore crab *Carcinus maenas* immunoreactive to crustacean hyperglycaemic hormone and its precursor-related peptide. *Cell Tiss. Res.* **300**, 193-205.

Weimann, J. M., Skiebe, P., Heinzel, H-G., Soto, C., Kopell, N., Jorge-Rivera, J. C. and Marder, E. (1997). Modulation of oscillator interactions in the crab stomatogastric ganglion by crustacean cardioactive peptide. *J. Neurosci.* **17**, 1748-1760.

Weimann, J. M., Marder, E., Evans, B. and Calabrese, R. L. (1993). The effects of SDRNFLRFNH2 and TNRNFLRFNH2 on the motor patterns of the stomatogastric ganglion of the crab, *Cancer borealis*. *J. Exp. Biol.* **181**, 1-26.

Wood, D. E., Nishikawa, M. and Derby, C. D. (1996). Proctolin-like immunoreactivity and identified neurosecretory cells as putative substrates for modulation of courtship display behavior in the blue crab, *Callinectes sapidus*. *J. Comp. Neurol.* **368**, 153-163.

Worden, M. K., Kravitz, E. A. and Goy, M. F. (1995). Peptide F1, an N-terminally extended analog of FMRFamide, enhances contractile activity in multiple target tissues in lobster. *J. Exp. Biol.* **198**, 97-108.

Yang, W. J., Aida, K. and Nagasawa, H. (1999). Characterization of chromatophorotropic neuropeptides from the kuruma prawn *Penaeus japonicus*. *Gen. Comp. Endocrinol.* **114**, 415-424.